A study of Giant Graviton Dynamics in the Restricted Schur Polynomial Basis

Vincent De Comarmond

A dissertation submitted to the Faculty of Science,
University of the Witwatersrand, Johannesburg,
in fulfilment of the requirements for the degree of Master of Science.

Supervisor: Professor Robert de Mello Koch

January 2011, Johannesburg

Declaration

I declare that this dissertation is my own, unaided work. It is being submitted for the Degree of Master of Science in the University of the Witwatersrand, Johannesburg. It has not been submitted before for any degree or examination in any other University.

Hamand

(Signature of Candidate)

7th day of July 2011

Abstract

Anomalous dimensions are calculated for a certain class of operators in the restricted Schur polynomial basis in the large N limit. A new computationally simple form of the dilatation operator is derived and used in this dissertation. The class of operators investigated have bare dimension of $\mathcal{O}(N)$. Thus the calculation necessarily sums non-planar Feynmann diagrams as the planar approximation has broken down for operators of this size. The operators investigated have two long columns and the operators mix under the action of the dilatation operator, however the mixing of operators having a different number of columns is suppressed and can be neglected in the large N limit. The action of the one loop dilatation operator is explicitly calculated for the cases where the operators have two, three and four impurities and it is found that in a particular limit the action of the one loop dilatation operator reduces to that of a discrete second derivative. The lattice on which the discretised second derivative is defined is provided by the Young tableaux itself. The one loop dilatation operator is diagonalised numerically and produces a surprisingly simple linear spectrum, with interesting degeneracies. The spectrum can be understood in terms of a collection of harmonic oscillators. The frequencies of the oscillators are all multiples of $8g_{YM}^2$ and can be related to the set of Young tableaux acted upon by the dilatation operator. This equivalence to harmonic oscillators generalises on previously found results in the BPS sector, and suggests that the system is integrable. The work presented here is based primarily on research carried out by R.de Mello Koch, V De Comarmond, and K. Jefferies in [1].

Acknowledgements

I would like to thank my supervisor Prof. Robert de Mello Koch, for all the effort he has put in over the years. My parents and my brother. Further I'd like to thank all my friends who supported me over the years, and everyone who has helped me reach this point. I'd also like to thank the National Institute for Theoretical Physics (NITheP) and the National Research Foundation (NRF) for their financial support. Finally I'd like to thank my God.

Contents

List of Figures

Part I

Background

Chapter 1

Introduction

1.1 An overview

The dilatation operator (as calculated to two loops in [2]) allows for the calculation of anomalous dimensions in a Conformal Field Theory (CFT). Further, the Anti-de Sitter/Conformal Field Theory (AdS/CFT) correspondence [3, 4, 5] can then be used to relate the anomalous dimensions of the Conformal Field Theory to energies in the dual string theory. For operators of large bare dimension ($\mathcal{O}(\sqrt{N})$ or larger) the calculation of the action of the dilatation operator is not trivial, as the planar approximation breaks down. The presented research investigates the anomalous dimension of a system of operators with bare dimension $\mathcal{O}(N)$. These operators can be related to the giant gravitons of [6], as suggested in [7, 8] following work done in [9].

Further the operators studied are composed of more than a single type of matrix. It is therefore clear that the techniques used must deal with multi-matrix dynamics in the (non-planar) large N limit efficiently. Such techniques have been recently developed in [8, 10, 11, 12, 13, 14, 15]. As the presented work was done in the large N limit, some simplification is expected (see [16] for discussion on this point) and indeed the resulting spectrum in simple even away from the BPS sector. This result is significant in that it suggests that the spectrum is both genuinely simple and may be simply understood without using facts implied by supersymmetry.

Using Schur Polynomial technology (discussed effectively in [8, 10, 11, 13, 17, 18]), we have been able to calculate the anomalous dimensions of a certain class of operators with bare dimension of $\mathcal{O}$(N) containing three and four impurities in the large N limit, thus extending upon the work presented in [18]. The results we obtain, together with those found in [18] allow a simple ansatz to be made for a more general case where the operators have an arbitrary number of impurities. In pursuing this end, we were also able to derive a new, computationally easier form for the Dilatation operator, marking a departure in approach from the more cumbersome approach used in [11, 12, 13, 18].

Finally it should be noted that work limited to the BPS sector has been carried out in [19, 20, 21, 22, 23, 24], and where the results coincide they agree. Our study [1] differs from these in that the presented spectra do not describe the entire set of BPS operators (where different BPS states may not have a simple dual interpretation), but instead focus on a specified set of operators that form a decoupled sector at large N.

1.2 Outline

The rest of this chapter (Chapter 1) introduces some of the background concepts needed for the rest of the work. Chapter 2 deals with giant gravitons, the objects studied in this dissertation. Chapter 3 deals with multi-matrix models, and also discusses the breakdown of the planar approximation. Chapter 3 thus explains why in order to capture the large N limit one needs to do more than just sum the planar Feynmann diagrams. Chapter 4 discusses Schur polynomials and Schur polynomial technology, which were used extensively in the research presented in this dissertation. Chapter 5 presents a derivation for the new form of the dilatation operator used in the research. Chapter 6 discusses the projectors arising in Chapter 5. Chapter 7 looks at spectra obtained for various classes of operator (operators built with two, three and four impurities respectively) and limiting cases of the action of the dilatation operator obtained. Chapter 8 discusses the results found in the research. Appendix A gives explicitly the results for the action of the dilatation operator on the states involved. Appendix B and Appendix C elucidate some details neglected in Chapter 5 and Chapter 6.

Appendix D gives a representation of the group elements of S_4, as needed for an example Chapter 4.

1.3 String theories and Conformal Field theories

During the 20^{th} century two prominent theories of physics were born and took shape, namely General Relativity (GR) and Quantum Field theory (QFT), both of which are still active areas of research . GR is a classical theory concerning the fundamental "force" of gravity. Attempts to quantise GR have so far not been successful due to the (apparent) non-renormalisability of the theory, thus GR is "stuck" in the classical realm and cannot describe physics at the quantum level.

The Standard Model (the most accurate physical theory produced to date) is an example of a QFT. Produced somewhat later in the 20^{th} century, QFTs are able to effectively describe the electromagnetic force, weak force and strong force in a unified way. Admittedly however the strong force is still an area of much difficulty. QFTs however good suffer from a number of problems, one of which is the inability of QFTs to correctly describe quantum corrections to gravitational interactions.

One may ask where the problem lies if we have two theories which adequately describe all four fundamental forces with acceptable accuracy? The problem arises in the fact that the theories are incompatible in physically realizable situations where neither gravitational effects or quantum effects are negligible, such as the early universe or the final stages of black hole evaporation. This problem of incompatibility has led to the development of string theory. String theory is arguably the most promising candidate for a theory of quantum gravity which also incorporates the other fundamental forces.

Conformal field theories are QFTs that are invariant under conformal transformations. The conformal transformations refer to dilatations (a dilatation is a rescaling of the metric), Poincaré transformations and special conformal transformations. It is believed that an invariance under dilatations implies an invariance under special conformal transformations, as whenever one has been found so has the other, however this has yet to be proved. Invariance under special conformal transformations guarantees invariance under dilatations. In total then CFTs are QFTs that are invariant under conformal transformations and which may also have conserved fermionic supercharges.

1.4 The AdS/CFT correspondence

This section is by no means meant to be a comprehensive review of the AdS/CFT correspondence. The purpose of this section is merely to highlight the existence of the conjecture which is used in the interpretation of the results. The conjecture by J.M. Maldacena is effectively dealt with and developed in [3, 4, 5] to which the reader is referred.

1.4.1 Anti de Sitter Space

Before one considers the actual conjecture, one must understand what is meant by 'Anti de Sitter' space and 'Conformal field theory' . Anti de Sitter space is the maximally symmetric solution to the Einstein equation with an attractive cosmological constant. Thus Anti de Sitter space has a constant negative curvature. Of particular interest in this dissertation is the space $AdS_5 \times S^5$, so this will be used as an example. First consider the space AdS_5, this is most easily done by considering a 5-dimensional hyper-surface embedded in a 6 dimensional space, the hyper-surface satisfies the equation:

$$-X_0^2 - X_5^2 + X_1^2 + X_2^2 + X_3^2 + X_4^2 = -R^2 \tag{1.1}$$

Where R is a constant. The metric of the 6 dimensional ambient space is given by:

$$ds^2 = -dX_0^2 - dX_5^2 + dX_1^2 + dX_2^2 + dX_3^2 + dX_4^2 \tag{1.2}$$

Parametrise the hyper-surface by $\vec{x}$,t and u as follows $(i = 1, 2, 3)$:

$$X_0 = \frac{1}{2u}(1 + u^2(\vec{x} \cdot \vec{x} - t^2) + u^2R^2) \tag{1.3}$$

$$X_i = Rux^i \tag{1.4}$$

$$X_4 = \frac{1}{2u}(1 + u^2(\vec{x} \cdot \vec{x} - t^2) - u^2R^2) \tag{1.5}$$

$$X_5 = Rut \tag{1.6}$$

Note that when $u = 0$ the co-ordinates induced on the hyper-surface are singular. The hyperplane defined by $u = 0$ ($X_0 = X_4$) divides the space into a region covered by co-ordinate chart where $u > 0$ and a region covered by a co-ordinate chart where $u < 0$. For the following the co-ordinate chart defined by $u > 0$ (which only covers half of AdS_5) is chosen. This parametrisation induces the following metric on the hyper-surface:

$$ds^2 = R^2(u^2(-dt^2 + dx^i \cdot dx^i) + \frac{du^2}{u^2}) \tag{1.7}$$

Let us examine some of the features of the above metric. At $u = 0$ one finds a horizon. At $u = \infty$ there is a boundary (i.e. at $u = \infty$ the proper length does not increase if u increases). The metric at the boundary can be thought of as follows:

$$ds^2 = K^2(-dt^2 + d\vec{x} \cdot d\vec{x}) \tag{1.8}$$

Notice that, as K is just some constant, the metric identifies the $3+1$ dimensional boundary space as Minkowski spacetime. The next property of the space to examine is the curvature. The Ricci tensor is most easily calculated with a further co-ordinate change, in which $u = 1/z$ and R is set equal to 1. The resulting co-ordinates describe the Poincaré patch , which covers the half-space defined by $z > 0$. The metric is given by :

$$ds^2 = \frac{1}{z^2}(-dt^2 + d\vec{x} \cdot d\vec{x} + dz^2) \tag{1.9}$$

Calculating the Ricci tensor and scalar leads to the following results:

$$\mathbf{R}_{\mu\nu} = -4g_{\mu\nu} \tag{1.10}$$

$$\mathbf{R} = -20 \tag{1.11}$$

Whilst for an Anti de Sitter space of arbitrary dimension (AdS_d) the following results are found:

$$\mathbf{R}_{\mu\nu} = -(d-1)g_{\mu\nu} \tag{1.12}$$

$$\mathbf{R} = -d(d-1) \tag{1.13}$$

The aforementioned constant negative curvature of the space is apparent.Consider the vacuum Einstein equation with a cosmological constant.

$$\mathbf{R}_{\mu\nu} - \frac{1}{2}\mathbf{R}g_{\mu\nu} + \Lambda g_{\mu\nu} = 0 \tag{1.14}$$

Inserting the above expressions for $\mathbf{R}_{\mu\nu}$ and $\mathbf{R}$, and re-inserting the radius of curvature R, one finds:

$$\Lambda = -\frac{(d-1)(d-2)}{2R^2} \tag{1.15}$$

Above the S^5 part of $AdS_5 \times S^5$ has been neglected. The S^5 in $AdS_5 \times S^5$ represents a further compact space (a 5-sphere) at each point in the AdS space. In essence each point in the AdS space is supplemented by a sphere. The 5 sphere satisfies:

$$(x^1)^2 + (x^2)^2 + (x^3)^2 + (x^4)^2 + (x^5)^2 + (x^6)^2 = R^2 \tag{1.16}$$

Where R is the same constant as used in (1.1).

1.4.2 The conjecture

The following is a heuristic explanation of Maldacena's conjecture [3]. Building on previously calculated results, Maldacena showed that in the large N limit, the Hilbert space of states of certain CFTs contained states describing quantum gravity on $AdS \times C$ [1] spacetimes. This led him to conjecture that: "*Type IIB string theory on $AdS_5 \times S^5$ plus some appropriate boundary conditions (and possibly also some boundary degrees of freedom) is dual to $N = 4$ $d = 3{+}1$ $U(N)$ super-Yang-Mills.*". This is not the most general statement of the conjecture, but it is the form of the conjecture which is most relevant for this dissertation.

The conjecture as written above is rather abstract. The following argument by Klebanov (see [25]) provides a physical picture for the conjecture. This argument is based on a detailed calculation (see [26, 27]) which provided motivation for Maldacena's conjecture. Gravitons (closed strings) are scattered from a stack of $D3$ branes in the low energy limit. This calculation can be done in $\mathcal{N} = 4$ SYM, where the $D3$ branes couple to a 4-form gauge potential. If the number of branes is sufficiently large, the brane stack can be treated as a heavy object which will deform the background space in a theory of gravity. In this case gravitons scattering of the $D3$ brane stack can be seen as gravitons scattering from a heavy object in $3+1$ dimensions (a black hole). The calculations are done and provided the brane stack is sufficiently heavy to deform the

[1] Here C is a compact space

background space the results of the calculations should agree. This idea leads to the following picture:

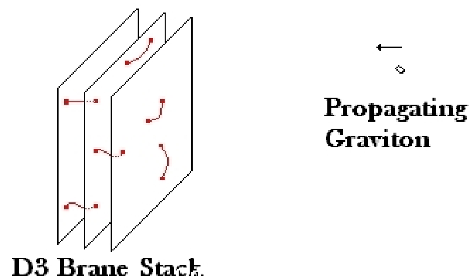

Figure 1.1: Graviton scattering off a stack of D3 branes

The action for the above picture is given by:

$$S_{int} + S^{3+1}_{\mathcal{N}=4\text{SYM}} + S^{\text{flat space 9+1}}_{\text{IIB supergravity}} \tag{1.17}$$

The S_{int} term vanishes in the low energy limit. $S^{3+1}_{\mathcal{N}=4\text{SYM}}$ is the Super Yang-Mills term of the action which describes the low energy dynamics of the branes. The $S^{\text{flat space 9+1}}_{\text{IIB supergravity}}$ term is the action for the gravitons away from the branes.

In the other picture (i.e. gravitons scattering of a black hole) one finds:

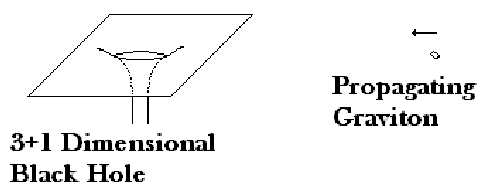

Figure 1.2: Graviton scattering off a Black hole

The action for the above picture is given by:

$$S^{\text{Near } D3 \text{ horizon geometry}}_{\text{IIB string}} + S^{\text{flat space 9+1}}_{\text{IIB supergravity}} \tag{1.18}$$

Only the near-horizon geometry is important as only strings in the near horizon geometry will be redshifted to such an extent that they survive the low energy limit. Equating the two pictures, it becomes obvious that the flat-space supergravity term agrees on both sides. If the two pictures really agree, then for equivalence, it is required that:

$$S_{\text{IIB string}}^{\text{Near } D3 \text{ horizon geometry}} = S_{\mathcal{N}=4\text{SYM}}^{3+1} \tag{1.19}$$

This leads to the conjecture that a string theory in AdS space is equivalent to a Conformal field theory on the boundary of the space. The above details in particular are for the claimed equivalence between type IIB string theory in $AdS_5 \times S^5$ and $\mathcal{N} = 4$ SYM (Super Yang-Mills) on the Minkowski boundary space. However the conjecture extends to the other theories of quantum gravity in Anti de Sitter space and supersymmetric Conformal field theories on the boundaries of these AdS spaces . This conjecture has been very well tested and has never been found to be wrong, see [28] and references therein for example.

In fact the evidence for this conjecture is so overwhelming that one may wonder why no proof has been found - the reason may be the strong/weak coupling duality. The strong-weak coupling duality makes the AdS/CFT conjecture very useful for applications, but also creates technical difficulties in proving the correspondence. Upon a closer investigation (of the AdS/CFT correspondence), it is found that:

$$g_s = g_{YM}^2 \qquad \frac{R^2}{l_s^2} = \sqrt{g_{YM}^2 N} \tag{1.20}$$

Here g_s is the string coupling, g_{YM} is the Yang-Mills coupling, l_s is the string length and N is the rank of the SYM gauge group. R is the radius of curvature of the AdS_5 and S^5 spaces in $AdS_5 \times S^5$.

The strong-weak coupling nature of the duality is easily understood in terms of the second relation, where the parameters l_s and N are fixed at some finite value. Where the CFT is strongly coupled and may not be perturbatively treated, the radius of curvature of the $AdS_5 \times S^5$ space is large (i.e. the spacetime is nearly flat) and the supergravity approximation is justified. Where the radius of curvature of the $AdS_5 \times S^5$ space is small (i.e. the spacetime is highly curved) and the supergravity description is no longer valid, the Yang-Mills coupling is small and may be treated perturbatively. Hence proving the correspondence is technically difficult as any calculation is always difficult on at least one side of the correspondence. In addition to the mentioned technical difficultly there may well be other difficulties both conceptual and technical which will make proving the AdS/CFT correspondence very difficult.

For the correspondence to be useful a dictionary relating objects in the Conformal Field theory to objects in the dual string theory is needed (see [4, 5]). Such a dictionary is under development, and it is this dictionary-in-progress with which applications of the correspondence are being investigated. One may hope that eventually a complete translation between the theories will be possible, but presently the correspondence is not understood well enough for this to be possible.

1.4.3 Relating the conformal dimension in a CFT to energies in quantum gravity

Relating anomalous dimensions of operators in $\mathcal{N} = 4$ SYM to energies in type IIB string theory is important for the correct interpretation of the results of the work covered in this dissertation. It is not difficult to appreciate the importance of anomalous dimensions in a CFT.

In a QFT the basic observable is the S-matrix. In a CFT however the S-matrix is not an observable, as is explained below. In a QFT a rough procedure for scattering is as follows:

1. Observe non-interacting single particle states in the far past.
2. Allow the particles to scatter off one another at some future time.
3. Wait a very long time before observing single particle states in the far future.

This procedure is possible, because one can separate the single-particle states out from the multi-particle states and the vacuum state. This is done using the LSZ Reduction formula (see [29], however this is treated in many standard QFT texts). This procedure fails in a CFT due to the inability to separate out single-particle states using a LSZ-type reduction. Single-particle states cannot be separated out in a CFT as there is no gap in the spectrum between the vacuum state and the single-particle states, making it impossible to isolate the single-particle states. The general heuristic argument given for this failure follows: Recall that a Conformal Field theory is invariant under conformal transformations. Among the conformal transformations there are dilatations, which re-scale the metric of the theory. If this is the case, then the concept of a "far past" or "far future" is not sensible, as if an event is described as being in the distant past for example, the metric can always be re-scaled so that the event appears to occur in the near past. Further, under this re-scaling of the metric, none of the physics changes (i.e. the action is invariant), hence there is no sensible concept of single-particle states in the far past/future.

This begs the question: what exactly is a good observable in a CFT? To answer this one can consider the form of the two-point correlation function in a Conformal Field theory, the form of which is fixed by the requirement of conformal invariance. The two-point function in a CFT is given by (See [2, 30]):

$$\langle \mathcal{O}_a(\overrightarrow{x})\mathcal{O}_b(\overrightarrow{y})\rangle = \frac{\delta_{ab}}{|\vec{x}-\vec{y}|^{2\Delta_a}} \tag{1.21}$$

Here it is assumed that the operators have well-defined scaling dimensions. The quantity Δ_a is the conformal dimension of the operators involved. The anomalous dimension, unlike the S-matrix, is a good observable in a CFT (the next section explains how the anomalous dimension is obtained) .

As already stated the AdS/CFT correspondence relates a string theory in AdS space to a CFT on the boundary of the space. As claimed in the title of this chapter, anomalous dimensions in the CFT can be related to energies in the string theory. Here is a brief overview of how this is done in the case of interest (type IIB string theory in $AdS_5 \times S^5$ and $\mathcal{N} = 4$ SYM). Recall that $\mathcal{N} = 4$ SYM lives in $3 + 1$ dimensional Minkowski space. Consider the metric for Minkowski spacetime:

$$ds^2 = -dt^2 + d\vec{x} \cdot d\vec{x} \tag{1.22}$$

Euclideanise, by making use of the transformation: $t = ix_4$

$$\Rightarrow ds^2 = dx_4^2 + d\vec{x} \cdot d\vec{x} \tag{1.23}$$

Change to spherical co-ordinates, to give:

$$ds^2 = dr^2 + r^2 d\Omega_3^2 \tag{1.24}$$

Letting $r = e^\tau$ results in:

$$ds^2 = e^{2\tau}(d\tau^2 + d\Omega_3^2) \tag{1.25}$$

A conformal transformation is performed to eliminate $e^{2\tau}$.

Giving:

$$ds^2 = d\tau^2 + d\Omega_3^2 \tag{1.26}$$

which is the metric of the $\mathbb{R} \times S^3$ boundary of the AdS_5 space where the IIB string theory is defined.

To see the relation, recall that energy is the conserved charge associated with invariance under time translations. Further note that the Hamiltonian operator is nothing more than the generator of time translations. So given a system which is invariant under time translations, the Hamiltonian gives a conserved energy. Thus:

$$H = i\frac{\partial}{\partial t} \to E. \tag{1.27}$$

Under a time translation ($\tau \to \tau + a$) on the string theory side of the correspondence (i.e. on the boundary metric of the AdS_5 space (1.26)), one finds the following on the CFT side of the correspondence:

$$\begin{aligned} &r = e^{\tau} \\ &\tau \to \tau + a \\ &\Rightarrow r \to e^{a} r \end{aligned} \tag{1.28}$$

But $r \to e^a r$ is just a conformal transformation (specifically a re-scaling). Hence, time translations on the AdS side of the correspondence, as generated by the Hamiltonian, are directly related to scale transformations on the CFT side of the correspondence. The generator of this conformal transformation is the dilatation operator (this is discussed in the following section).

Although the above dealt mostly with type IIB string theory (on $AdS_5 \times S^5$) and $\mathcal{N} = 4$ Super Yang-Mills, the following general comments can be made (see [31]):

- The Hamiltonian of the string theory (on the AdS side of the correspondence) is related to the Dilatation operator of the Conformal field theory on the boundary of the AdS space.
- Energies in the string theory (eigenvalues of the Hamiltonian) are related

to conformal dimensions of the CFT (which are eigenvalues of the Dilatation operator).

1.4.4 The dilatation operator

The spectrum of conformal dimensions is given by the eigenvalues of the dilatation operator. The dilatation operator itself can be calculated order by order in $\hbar$ following the expansion[2] (see [2] in particular, see also[30] for details):

$$\mathcal{D} = \sum_{j=0}^{\infty} (\frac{g_{YM}^2}{16\pi^2})^j \mathcal{D}_{2j} = \mathcal{D}_0 + \frac{g_{YM}^2}{16\pi^2}\mathcal{D}_2 + \cdots \tag{1.29}$$

In [2, 30] the $\mathcal{D}_0, \mathcal{D}_2$ and $\mathcal{D}_4$ contributions to the dilatation operator are given. In the $SU(2)$ sector[3], the $\mathcal{D}_0$ and $\mathcal{D}_2$ contributions are given by :

$$\mathcal{D}_0 = Tr\big(Y\frac{d}{dY}\big) + Tr\big(Z\frac{d}{dZ}\big) \tag{1.30}$$

$$\mathcal{D}_2 = -Tr\big([Y,Z][\frac{d}{dY}, \frac{d}{dZ}]\big) \tag{1.31}$$

Here Y and Z are the charged scalar fields of $\mathcal{N} = 4$ SYM (for a discussion on the charged scalar fields of $\mathcal{N} = 4$ SYM the reader is refered to Chapter 3.3). The tree level contribution is easily understood. Consider the tree level conribution to the dilatation operator acting on $Tr(Z^n)Tr(Y^m)$ for example:

$$\mathcal{D}_{\mathbf{0}} Tr(Z^n)Tr(Y^m) = \Big(Tr\big(Y\frac{d}{dY}\big) + Tr\big(Z\frac{d}{dZ}\big)\Big)Tr(Z^n)Tr(Y^m)$$

But $Tr\big(Z\frac{d}{dZ}\big)Tr(Z^n) = Z^{\mu}{}_{\nu}\frac{d}{dZ^{\mu}{}_{\nu}}Z^{\alpha}{}_{\beta}Z^{\beta}{}_{\gamma}\cdots Z^{\omega}{}_{\alpha}$

$$= Z^{\mu}{}_{\nu} \times (\delta^{\alpha}_{\mu}\delta^{\nu}_{\beta}Z^{\beta}{}_{\gamma}\cdots Z^{\omega}{}_{\alpha} + \cdots + Z^{\alpha}{}_{\beta}Z^{\beta}{}_{\gamma}\cdots\delta^{\omega}_{\mu}\delta^{\nu}_{\alpha})$$

$$= nTr(Z^n)$$

So by extension

$$\mathcal{D}_{\mathbf{0}} Tr(Z^n)Tr(Y^m) = (n+m)Tr(Z^n)Tr(Y^m) \tag{1.32}$$

---

[2]Here it must be born in mind that the Yang-Mills coupling enters the action in much the same way that $\hbar$ does. Explicitly g_{YM}^2 enters the action where $\hbar$ does and plays the role of $\hbar$ in the expansion.

[3]The $SU(2)$ sector of $\mathcal{N} = 4$ SYM is the simplest non-trivial sector, in which the operators are restricted to contain only two types of complex scalar fields Y and Z (more details about the $SU(2)$ sector can be found in [32] and references therein).

Therefore the tree level contribution just counts the (classical) power of the matrix fields. Further in $3+1$ dimensions $[Z] = [Y] = L^{-1}$, thus $\mathcal{D}_0$ gives the correct classical dimension. The higher order contributions (in g_{YM}^2) to $\mathcal{D}$ account for the changes to this power due to quantum effects (wave function renormalization), these are less easily understood (see [2, 30]for effective treatment). Of particular interest for this dissertation is the contribution from $\mathcal{D}_2$. The eigenvalues of $\mathcal{D}_2$ give the one loop contribution to the anomalous dimensions of the operators acted upon by $\mathcal{D}_2$.

Chapter 2

Giant Gravitons

This chapter gives a review of the work done in [6], wherein giant gravitons are introduced, providing a physical model for the stringy exclusion principle, which limits the angular momentum on the compact spherical component of the $AdS \times S$ space. Here the focus will be on the $AdS_5 \times S^5$ case (although the analysis follows closely that of the $AdS_7 \times S^4$ case done in detail in [6]).

Note : This chapter focusses nearly exclusively on sphere giants, however there is another species of giant graviton, the AdS giant. AdS giant gravitons were brought to light in [33, 34], however they are not of significant interest in this dissertation. Throughout any reference to giant gravitons or giants should be interpreted as sphere giants. AdS giants will always be referred to by their full name in this dissertation.

2.1 A simple analogy

The following classical analogy provides a good demonstration of the logic behind the calculation. Consider a dipole, where the two opposite charges are connected by a spring and the dipole is allowed to move in some Euclidean plane. Let the centre of mass of the dipole have some definite momentum and let a constant magnetic field pass through the Euclidean plane. Assume the dipole does not spin about its own centre of mass. A classical analysis would suggest that the force from the magnetic field on either side of the dipole is:

$$\vec{F} = q\vec{v} \times \vec{B} \tag{2.1}$$

As the particles on the opposite side of the dipole have opposite charge and the charges move together (i.e. in the same direction), the above magnetic contribution to the force would tend to pull the charges constituting the dipole further apart. However as the spring connecting the two charges of the dipole together stretches, the force it exerts on the two particles increases. This picture would then suggest that the dipole stretches with increasing momentum until equilibrium is reached between the force due to the magnetic field and the spring force (for simplicity, the force of electric attraction between the opposite ends of the dipole is neglected).

In the above case, the dipole was placed on an Euclidean plane. However, it is possible to create similar conditions on a sphere. To achieve this the dipole is placed on a 2-sphere with the charges constrained to move on the sphere, the spring lying on the chord connecting the two charges. Place a magnetic monopole at the centre of the sphere in order to provide the sphere with N units of magnetic flux. Allowing the dipole to move on the surface of the sphere will produce the same effects as above, i.e. the spring connecting the charges will stretch with increasing angular momentum. There is however a fundamental difference in this case, in that the opposing charges are now limited in their distance of separation. At maximum separation the opposing charges lie on opposite ends of the 2-sphere and the spring is stretched to its maximum length. Further, at this point the dipole has the maximum angular momentum allowable by the system. This suggests that a limit on the size of the dipole is related to the maximum angular momentum the dipole can reach. A careful analysis shows that this is indeed the case and further, the maximum allowable angular momentum is dependent on the strength of the magnetic monopole placed at the centre of the sphere.

2.2 Sphere Giants in $AdS_5 \times S^5$

Bearing the result of the above analogy in mind, the following analysis of the motion of a BPS particle on the S^5 component of $AdS_5 \times S^5$ can be carried out.

This analysis will be classical and will make the assumption that the radius of curvature of the 5-sphere is very much larger than the Planck length ($R \gg l_p$). Consider a 5-sphere with radius R, the angular contribution to the volume is given by $\Omega_5 = \frac{\pi^{5/2}}{\Gamma(7/2)}$. Introduce a 5-form field strength with flux density B. Flux quantization on the 5-sphere requires:

$$B\Omega_5 R^5 = 2\pi N \tag{2.2}$$

Where N is the number of flux quanta. We take the large N limit, keeping $g_s N$ fixed. From the supergravity equations of motion, it is found:

$$R = (4\pi g_s N)^{\frac{1}{4}} l_s \tag{2.3}$$

This results in :

$$B = \frac{N^{-\frac{1}{4}} l_s^{-5}}{2\Omega_5 (4\pi)^{\frac{1}{4}}} (g_s)^{-\frac{5}{4}} \tag{2.4}$$

Embedded in a 6-dimensional Euclidean space, the 5-sphere satisfies the equation:

$$X_1^2 + X_2^2 + X_3^2 + X_4^2 + X_5^2 + X_6^2 = R^2 \tag{2.5}$$

The co-ordinates $(\theta_1, \theta_2, \theta_3, \theta_4, \theta_5)$ parametrise the space conveniently and are related to the Euclidean space co-ordinates as follows:

$$\begin{aligned}
X_1 &= R\cos(\theta_1) \\
X_2 &= R\sin(\theta_1)\cos(\theta_2) \\
X_3 &= R\sin(\theta_1)\sin(\theta_2)\cos(\theta_3) \\
X_4 &= R\sin(\theta_1)\sin(\theta_2)\sin(\theta_3)\cos(\theta_4) \\
X_5 &= R\sin(\theta_1)\sin(\theta_2)\sin(\theta_3)\sin(\theta_4)\cos(\theta_5) \\
X_6 &= R\sin(\theta_1)\sin(\theta_2)\sin(\theta_3)\sin(\theta_4)\sin(\theta_5)
\end{aligned} \tag{2.6}$$

A $D3$ brane is embedded in the S^5 space and is the dipole for the problem, in that it has a non-zero dipole moment with respect to the 5-form field strength. Parametrise the surface of the $D3$ brane by the co-ordinates $\theta_3, \theta_4, \theta_5$. The brane in this case is free to move in the $X_1 - X_2$ plane. The size of the brane is given by:

$$\begin{aligned}
r^2 = X_3^2 + X_4^2 + X_5^2 + X_6^2 &= R^2 \sin^2(\theta_1)\sin^2(\theta_2) \\
\Rightarrow r &= R\sin(\theta_1)\sin(\theta_2)
\end{aligned} \tag{2.7}$$

Evidently, the size of the above brane, as given by r, satisfies the following:

$$\begin{aligned}
&R^2 - r^2 = X_1^2 + X_2^2 \\
&r \leq R \text{ with } r = R \text{ at } X_1 = X_2 = 0. \\
&\text{Hence } r = R \text{ at } \theta_1 = \theta_2 = \frac{1}{2}\pi.
\end{aligned} \tag{2.8}$$

The motion executed in the $X_1 - X_2$ plane can be conveniently parametrised by making one more co-ordinate change:

$$\begin{aligned}
X_1 &= \sqrt{R^2 - r^2}\cos(\phi) \\
X_2 &= \sqrt{R^2 - r^2}\sin(\phi)
\end{aligned} \tag{2.9}$$

The world-volume of the $D3$ brane is then fully described by r, ϕ, θ_3, θ_4 and θ_5, which are related to the Euclidean co-ordinates as follows:

$$\begin{aligned}
X_1 &= \sqrt{R^2 - r^2}\cos(\phi) \\
X_2 &= \sqrt{R^2 - r^2}\sin(\phi) \\
X_3 &= r\cos(\theta_3) \\
X_4 &= r\sin(\theta_3)\cos(\theta_4) \\
X_5 &= r\sin(\theta_3)\sin(\theta_4)\cos(\theta_5) \\
X_6 &= r\sin(\theta_3)\sin(\theta_4)\sin(\theta_5)
\end{aligned} \tag{2.10}$$

This parametrisation induces the following metric on the brane's world-volume.

$$\begin{aligned}
ds^2 &= \frac{R^2}{R^2 - r^2}dr^2 + (R^2 - r^2)d\phi^2 + r^2\big(d\theta_3^2 + \sin^2(\theta_3)d\theta_4^2 + \sin^2(\theta_3)\sin^2(\theta_4)d\theta_5^2\big) \\
\Rightarrow ds^2 &= \frac{R^2}{R^2 - r^2}dr^2 + (R^2 - r^2)d\phi^2 + r^2 d\Omega_3^2
\end{aligned} \tag{2.11}$$

The kinetic term of the Lagrangian can be found from the (Dirac-Born-Infeld) action, which is given by (see [35] for example):

$$S_{DBI} = -T_{m-2}\int \sqrt{|g|}d\tau d\sigma_1 \cdots d\sigma_{m-2} \tag{2.12}$$

Where $\tau, \sigma_1, \ldots, \sigma_{m-2}$ are world-volume co-ordinates and T is the brane tension. Thus the AdS term of the following metric is needed:

$$ds^2 = ds^2_{AdS_5} + ds^2_{S^5} \tag{2.13}$$

The metric for AdS_m (as given in [35]) is:

$$ds^2_{AdS_m} = -(1 + \frac{r^2_{AdS}}{\tilde{L}^2})dt^2 + \frac{dr^2_{AdS}}{1 + \frac{r^2_{AdS}}{\tilde{L}^2}} + r^2_{AdS} d\Omega^2_{m-2} \tag{2.14}$$

Here $\tilde{L}$ is the AdS scale and r_{AdS} is a non-negative radial co-ordinate. The classical stable solutions will be found where $r_{AdS} = 0$, this in turn sets $dt = d\tau$. By setting $r_{AdS} = 0$ and $dr_{AdS} = 0$ (this follows as r_{AdS} is set to a constant), it can be seen that the metric for the AdS term on the world-volume of the brane reduces to [1]:

$$ds^2_{AdS_m} \to -dt^2$$

The parameters describing the S^5 space are : $r, \phi, \theta_3, \theta_4, \theta_5$. Under the assumption that $r_{AdS} = 0$, the metric of the 10 dimensional spacetime:

$$ds^2 = ds^2_{AdS_5} + ds^2_{S^5}$$

becomes the following metric on $\mathbb{R} \times S^5$:

$$ds^2 = -dt^2 + (R^2 - r^2)d\phi^2 + r^2 d\Omega^2_3 + \frac{R^2}{R^2 - r^2} dr^2 \tag{2.15}$$

For the cases of interest for this dissertation, the size of the membrane is assumed to be constant so that the contribution to the kinetic energy from the term containing dr can be dropped [1]. Also the $D3$ brane is assumed to be moving in the $X_1 - X_2$ plane with constant angular velocity, independent of its position in S^5, so that $d\phi = \dot{\phi} dt$. This leads to the metric on the world-volume of the brane:

$$\begin{aligned} ds^2 &= -dt^2 + (R^2 - r^2)\dot{\phi}^2 dt^2 + r^2 d\Omega^2_3 \\ &= (-1 + (R^2 - r^2)\dot{\phi}^2)dt^2 + r^2 d\Omega^2_3 \end{aligned} \tag{2.16}$$

This metric can then be inserted into the Dirac-Born-Infeld action. To get the kinetic term of the Lagrangian, the proper-time integral in the Dirac-Born-Infeld action is ignored. This gives the following contribution to the kinetic term of the Lagrangian:

$$\mathcal{L}_{DBI} = -T_{D3}\sqrt{-1 + (R^2 - r^2)\dot{\phi}^2} r^3 \Omega_3 \tag{2.17}$$

[1] Here an ansatz is made at the level of the action. Technically this is not correct as it restricts the ways in which the action can be varied. Doing the analysis thoroughly it is found that the ansatz for the D3 brane world-volume is indeed correct.

The tension of the $D3$ brane is given by:

$$T_{D3} = \frac{1}{(2\pi)^3 l_s^4 g_s} \Rightarrow T_{D3}\Omega_3 = \frac{N}{R^4} \tag{2.18}$$

Inserting this result into (2.17) results in the final form of the kinetic term:

$$\mathcal{L}_{DBI} = -\frac{Nr^3}{R^4}\sqrt{-1 + (R^2 - r^2)\dot{\phi}^2} \tag{2.19}$$

As in the toy model, there is a background field to which the object of interest couples. In this case the background field is a 5-form field strength, the action of which is described by the Chern-Simons coupling. This term is given by:

$$S_{CS} = \int_{\substack{\text{world}\\ \text{volume}}} C = \int_{\Sigma} F \tag{2.20}$$

Following the generalized Stokes theorem, $F = dC$ is the 5-form flux and Σ is the manifold bounded by the surface swept out by the brane per orbit. Recall that the 5-form flux was constant. Thus:

$$S_{CS} = \int_{\Sigma} F = \int_{\Sigma} BdV = B \times Vol(\Sigma) \tag{2.21}$$

Note that the angular velocity of the brane in S^5 is constant, this means that the action can only be linearly dependent on the period. Thus :

$$\begin{aligned} \mathcal{L}_{CS} &= \frac{S_{CS}}{T} = S_{CS}\frac{\dot{\phi}}{2\pi} \\ \Rightarrow \mathcal{L}_{CS} &= B \times Vol(\Sigma)\frac{\dot{\phi}}{2\pi} \end{aligned} \tag{2.22}$$

As the metric (2.11) is diagonal, the volume element is trivial to find:

$$dV = Rr^3 dr d\phi d\Omega_3 \tag{2.23}$$

The manifold is bounded by the size of the $D3$ brane ($r : 0 \to r$), and one orbit is to be integrated over ($\phi : 0 \to 2\pi$).

$$\begin{aligned} Vol(\Sigma) = \int_0^{2\pi} d\phi \int_0^r dr \int_{S^3} d\Omega_3 Rr^3 &= \pi^3 Rr^4 \\ \Rightarrow Vol(\Sigma) &= \Omega_5 Rr^4 \end{aligned} \tag{2.24}$$

Hence the Chern-Simons term is given by:

$$\mathcal{L}_{CS} = \frac{\dot{\phi}}{2\pi} BRr^4\Omega_5 \tag{2.25}$$

Using the flux quantization condition (2.2) this can be reduced to:

$$\mathcal{L}_{CS} = N\dot{\phi}\frac{r^4}{R^4} \tag{2.26}$$

The total Lagrangian is then simply:

$$\begin{aligned} &\mathcal{L} = \mathcal{L}_{DBI} + \mathcal{L}_{CS} \\ &\Rightarrow \mathcal{L} = -\frac{Nr^3}{R^4}\sqrt{-1 + (R^2 - r^2)\dot{\phi}^2} + N\dot{\phi}\frac{r^4}{R^4} \end{aligned} \tag{2.27}$$

The angular momentum is conjugate to the angular velocity, so

$$L = \frac{d\mathcal{L}}{d\dot{\phi}} = \frac{r^3 N}{R^4}\frac{(R^2 - r^2)\dot{\phi}}{\sqrt{1 - (R^2 - r^2)\dot{\phi}^2}} + \frac{r^4}{R^4}N \tag{2.28}$$

The variables of the angular momentum are bounded as follows: $(0 \leq r \leq R)$ and $(0 \leq \dot{\phi}R \leq 1)$. It is found that the angular momentum is an increasing function of r . The maximum of the angular momentum is then found to occur when $r = R$:

$$L = L_{max} = N \text{ when } r = R \tag{2.29}$$

This solution is found to lie at a minimum of the energy, thus it represents a classically stable solution in which momentum cut-off arises in a natural way. For further details the reader is referred to [6].

2.3 Conclusion

The above picture of sphere giants (i.e. those giant gravitons which extend in the compact spherical S component of $AdS \times S$) gives rise to an angular momentum cut-off in a natural way. This can be related to the stringy exclusion principle, placing a natural limit on the angular momentum of the brane in the spherical S component of $AdS \times S$. The radius of the of the brane increases with increasing angular momentum until the radius of the brane is equal to the radius of the sphere containing it, achieving the cut off in angular momentum. The above physical picture is consistent with the BPS formula for the energy given the angular momentum.

This analysis is far from providing a satisfactory understanding for the stringy exclusion principle. This is because although for the sphere giants described above the cut-off on angular momentum appears in a natural way, this is not true for the other species of graviton. AdS giant gravitons, as well as point-like gravitons do not have a naturally appearing cut-off in angular momentum. Further all three types of gravitons have the same energy and preserve the same supersymmetries. How exactly the stringy exclusion principle arises in general is then unclear.

What is clear however is that for the case of sphere giants there is a cut-off on angular momentum, and the above model provides a clear picture for understanding these sphere giant gravitons.

2.4 A brief note on AdS Giants

The existence of AdS giants was brought to light in [33, 34]. AdS giants arise naturally from a very similar analysis to the one above, but with a key difference, in that the analysis is carried out for the BPS particle expanding in the AdS space as opposed to the spherical S component of $AdS \times S$. Further it is found that the AdS giants have the same quantum numbers as both the Kaluza-Klein gravitons as well as the spherical giants. The most significant difference between AdS giants and sphere giants is that whilst sphere giants are limited in size by the size of the sphere they inhabit, AdS giants are not limited in size and may therefore expand to any size. In turn this means that unlike spherical giants which have a cut-off on angular momentum, AdS giants do not have a limit for their angular momentum. There are further subtle differences between the two species of giant which will not be discussed here (details are given in [33, 34]).

Chapter 3

Matrix Models

3.1 Single Matrix Models

This chapter briefly reviews the concept of matrix models and the failure of the planar approximation, justifying the use of computational techniques such Schur polynomials.

Consider briefly the path-integral formulation of Quantum Field theory. Of central importance is the path integral:

$$\int\limits_{\substack{\text{All possible}\\ \text{paths}}} e^{iS} \tag{3.1}$$

where S is the classical action of the theory (or the classical action plus counter-terms in the case of renormalized perturbation theory). The fields considered may be scalar fields, vector fields or matrix fields. Matrix fields are of particular interest here, because certain matrix models (i.e. Quantum Field theories formed with matrix fields) have been shown to be equivalent to non-critical string theories (see [36]), and further it has been conjectured that a random matrix model formulation in [37] is equivalent to M-theory.

Given a matrix model one considers a partition function of the following form:

$$\mathcal{Z} = \int [dM] e^{-\alpha Tr(M^2) + S_{int}} \tag{3.2}$$

Here M refers to Hermitian $N \times N$ matrices unless otherwise specified. The essential part of the above integral is the Gaussian piece of the integral. The interaction term S_{int}, can be treated perturbatively. Hermicity implies the diagonal entries of the matrix M are real, thus there are N real diagonal entries. There are then $N^2 - N$ off-diagonal entries. The condition $M = M^\dagger$ relates the upper triangular piece of the matrix to the lower triangular piece of the matrix. Thus there are $\frac{1}{2}(N^2 - N)$ independent off-diagonal complex entries in M. Each of these complex entries can be written in terms of two real entries. In total then there are $N^2 - N$ real off-diagonal entries, and N real diagonal entries giving a total of N^2 integration variables for the integral over M. Thus:

$$[dM] = \prod_{i=1}^{N} dM^i{}_i \prod_{i<j}^{N} d(M^{\Re})^i{}_j d(M^{\Im})^i{}_j \tag{3.3}$$

Where $(M^{\Re})^i{}_j$ and $(M^{\Im})^i{}_j$ are the real and imaginary parts of the matrix M respectively. Further, $Tr(M^2) = M^i{}_j M^j{}_i$ is a sum over N^2 terms, as both the sum over the index i and j run over N values. Hence the following integral:

$$I = \int [dM] e^{-\alpha Tr(M^2)} \tag{3.4}$$

has N^2 integration variables, each one of which is a simple Gaussian integral. Hence:

$$I = \int [dM] e^{-\alpha Tr(M^2)} = [\int_{-\infty}^{\infty} dx e^{-\alpha x^2}]^{N^2} = \left(\frac{\pi}{\alpha}\right)^{N^2/2} \tag{3.5}$$

In order to perform a perturbative expansion of S_{int} a source term can be coupled to the matrix field so that a generating functional may be formed. The generating functional is then:

$$\mathcal{Z}[J] = \int_{-\infty}^{\infty} [dM] e^{-\alpha Tr(M^2) + Tr(JM)}. \tag{3.6}$$

It is found that:

$$-\alpha Tr(M^2) + Tr(JM) = -\alpha(M^i{}_j - \frac{1}{2\alpha} J^i{}_j)(M^j{}_i - \frac{1}{2\alpha} J^j{}_i) + \frac{1}{4\alpha} J^i{}_j J^j{}_i$$

$$\Rightarrow \mathcal{Z}[J] = e^{\frac{1}{4\alpha} Tr(J^2)} \int_{-\infty}^{\infty} [dM] e^{-\alpha Tr\left((M - \frac{1}{2\alpha} J)^2\right)}$$

Let $\tilde{M} = M - \frac{1}{2\alpha} J$

$$\Rightarrow \mathcal{Z}[J] = e^{\frac{1}{4\alpha} Tr(J^2)} \int_{-\infty}^{\infty} [d\tilde{M}] e^{-\frac{1}{2}\tilde{M}^2}$$

$$\Rightarrow \mathcal{Z}[J] = \left(\frac{\pi}{\alpha}\right)^{\frac{1}{2}N^2} e^{\frac{1}{4\alpha} Tr(J^2)} \tag{3.7}$$

The generating functional allows computation of correlators in a perturbative expansion. In the above example then, this makes objects such as:

$$\langle M^i{}_j M^k{}_l \rangle = \int_{-\infty}^{\infty} [dM] M^i{}_j M^k{}_l e^{-\alpha Tr(M^2)} \tag{3.8}$$

easily accessible. In general the theory should be normalized so that it can be sensibly interpreted. The correlator of the two matrix fields is then:

$$\begin{aligned} \langle M^i{}_j M^k{}_l \rangle &= \frac{\int [dM] M^i{}_j M^k{}_l e^{-\alpha Tr(M^2)}}{\int [dM] e^{-\alpha Tr(M^2)}} = \frac{1}{\mathcal{Z}[0]} \frac{d}{dJ^j{}_i} \frac{d}{dJ^l{}_k} \mathcal{Z}[J]|_{J=0} \\ \Rightarrow \langle M^i{}_j M^k{}_l \rangle &= \frac{1}{2\alpha} \delta^k_j \delta^i_l \end{aligned} \tag{3.9}$$

The following correlators are easily derived:

$$\begin{aligned} \langle Tr(M^2) \rangle &= \frac{N^2}{2\alpha} \\ \langle Tr(M^4) \rangle &= 2\frac{N^3}{(2\alpha)^2} + \frac{N}{(2\alpha)^2} \end{aligned} \tag{3.10}$$

3.2 The planar approximation and its limitations

Feynman diagrams can be defined for the above matrix model (this can be done for any matrix model). Matrices are 2-index objects, this should be apparent in the diagrams representing matrices. The operators may consist of matrix fields which have been traced over or matrix fields which have not been traced over, the distinction between these two classes of operator should be apparent in any assigned diagrammatic rule. Let a matrix be represented by:

Figure 3.1: Feynman diagram for a single matrix

The corresponding correlator is:

$$\langle M^i{}_j \rangle = 0 \tag{3.11}$$

The correlator $\langle M^i{}_j M^k{}_l \rangle$ has two matrices. The result of this correlator is a delta function which links the indices of these two matrices. These links will be represented by ribbons which connect pairs of indices, the Feynman diagram for $\langle M^i{}_j M^k{}_l \rangle$ follows:

Figure 3.2: Feynman diagram for correlator of two untraced matrix fields

The corresponding correlator is:

$$\langle M^i{}_j M^k{}_l \rangle = \frac{1}{2\alpha} \delta^k_j \delta^i_l \tag{3.12}$$

Note that the ordering of the indices is important, diagrammatically this is implemented by not allowing ribbons to twist. Further, the indices must be written in the order they appear in the correlator. For operators consisting of fields which are traced over, the summed indices are repeated. Repeated indices are to be connected above the horizontal (the horizontal here is defined as the line on which the points representing the indices lie), whilst indices which are set equal by delta functions are to be connected below the horizontal by ribbons. As an example consider the following Feynman diagram for $\langle Tr(M^2) \rangle$:

Figure 3.3: Feynman diagram for $\langle Tr(M^2) \rangle$

The corresponding correlator is:

$$\langle Tr(M^2) \rangle = \frac{N^2}{2\alpha} \tag{3.13}$$

The Feynman rule which gives results consistent with the path integral approach is given by:

$$\langle Tr(M^n)\rangle = \sum_{\text{Feynman diagrams}} \frac{N^{\text{number of closed loops}}}{(2\alpha)^{\text{number of ribbons}}} \tag{3.14}$$

For example, this rule reproduces the result for $\langle Tr(M^4)\rangle$.

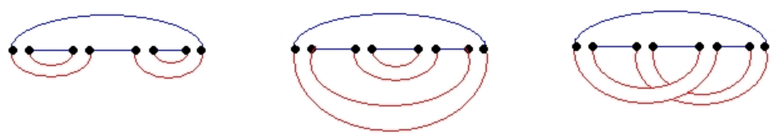

Figure 3.4: Feynman diagrams for $\langle Tr(M^4)\rangle$

Summing these Feynman diagrams reproduces:

$$\langle Tr(M^4)\rangle = 2\frac{N^3}{(2\alpha)^2} + \frac{N}{(2\alpha)^2} \tag{3.15}$$

To make connection to with $\mathcal{N} = 4$ SYM note that α as used above is given by: $\alpha = \frac{1}{g_{YM}^2} = \frac{N}{\lambda}$ in $\mathcal{N} = 4$ SYM. If N is very large, in particular in the 't Hooft limit ($N \to \infty$ and $\lambda = g_{YM}^2 N$ = a finite constant), the second term above can be neglected as it is damped by a factor of N^2 compared to the leading contribution. The diagram for the second term is actually topologically different to the diagrams summing to the first term. Particularly the diagrams corresponding to the first term can be drawn on a sphere, without the ribbons crossing. These diagrams are referred to as planar, meaning that they can be properly drawn on a flat plane.

The diagram corresponding to the second term however cannot be properly drawn on a plane as the ribbons cross. To be properly represented the ribbons must lie on different surfaces so that they do not cross one another. Any surface on which the ribbons can be drawn without crossing cannot be a sphere, such surfaces are referred to as non-planar. A torus is the lowest genus space needed for a proper representation of the diagram corresponding to the second term. A torus is a genus 1 space, effectively this means that the space has 1 “handle”. Further investigation shows that suppression of the non-planar diagrams can be related to the lowest genus space on which they can be properly drawn. Given a correlator, the Feynman diagrams which can be properly drawn on a space of lowest genus h are suppressed by a factor of N^{-2h} in comparison to the planar Feynman diagrams in the perturbative series for the correlator.

The basis of the planar approximation is then that in the 't Hooft limit, the non-planar diagrams are heavily suppressed (by at least a factor of N^2, where N is large), and hence can be neglected. Caution however, is needed when using the planar approximation, as the 't Hooft limit by itself does not guarantee the applicability of the planar approximation. Although the non-planar diagrams are suppressed, where the number of non-planar diagrams is very large, the combinatorial factor which arises from adding all the non-planar diagrams together can overwhelm the suppression. Indeed, when dealing with operators built using a large number of fields (large in that the number of traced matrix fields is of $\mathcal{O}(\sqrt{N})$ or more) the planar approximation breaks down because the number of non-planar diagrams that can be drawn far outnumbers the number of planar diagrams that can be drawn. Then even though each non-planar diagram is suppressed, the total contribution of the non-planar diagrams cannot be neglected.

3.3 The Matrix Fields X, Y and Z of $\mathcal{N} = 4$ Super Yang-Mills

Recall the S^5 component of $AdS_5 \times S^5$ exhibited $SO(6)$ isometry (the metric on the S^5 component of $AdS_5 \times S^5$ is invariant under $SO(6)$ transformations). This is seen as follows: the $SO(6)$ isometry group is the group of rotations in a six dimensional Euclidean space. The hyper-surface satisfying:

$$(x^1)^2 + (x^2)^2 + (x^3)^2 + (x^4)^2 + (x^5)^2 + (x^6)^2 = R^2 \tag{3.16}$$

defines S^5 in an ambient six dimensional Euclidean space. Clearly then S^5 exhibits $SO(6)$ isometry as the six dimensional Euclidean space exhibits $SO(6)$ isometry and the hypersurface described by (3.16) is invariant under $SO(6)$ transformations. An equivalent Conformal Field theory ($\mathcal{N} = 4$ SYM) should exhibit the same symmetries as the theory of gravity (IIB string theory) it is dual to.

The six Higgs fields $(\phi^1, \phi^2, \phi^3, \phi^4, \phi^5, \phi^6)$ of $\mathcal{N} = 4$ Super Yang-Mills exhibit $SO(6)$ R-symmetry. It is however convenient to complexify these fields as follows:

$$\begin{aligned} X &= \phi^1 + i\phi^2 \\ Y &= \phi^3 + i\phi^4 \\ Z &= \phi^5 + i\phi^6. \end{aligned} \tag{3.17}$$

The X, Y and Z fields exhibit $SU(4)$ symmetry. The group $SU(4)$ is a double cover of $SO(6)$, however the Lie algebras $su(4)$ and $so(6)$ are the same. The X,Y and Z fields are the fields of interest in this dissertation, where X,Y and Z belong to the complexified Lie algebra.

Chapter 4

Schur Polynomials

4.1 Schur Polynomials and restricted Schur Polynomials defined

Following work done in [9], Schur Polynomials were proposed in [7, 8] as field theory operators dual to sphere giants, AdS giants and composites of giants with Kaluza-Klein states. Restricted Schur polynomials (introduced in [11]) are a generalisation of the Schur polynomials, the properties of which are investigated in detail in [10, 11, 12, 13, 17]. The Schur polynomials are constructed to diagonalise the two-point correlation function in the free field theory (for a detailed proof of this see [8]). Schur Polynomials are defined as follows:

$$\chi_R(Z) = \frac{1}{n!}\sum_{\sigma\in S_n}\chi_R(\sigma)Z^{i_1}_{i_{\sigma(1)}}Z^{i_2}_{i_{\sigma(2)}}\cdots Z^{i_n}_{i_{\sigma(n)}} \tag{4.1}$$

This definition has many subtleties which only become apparent after examining the definition term by term as is done below.

If the Schur polynomial is evaluated over $SU(N)$, then one would interpret $\chi_R(U)$ on the left hand side above as the character of $U \in SU(N)$ in the irreducible representation R of $SU(N)$. However here $\chi_R(Z)$ is considered where Z is an element of the algebra $su(N)$, rather than the $SU(N)$ group. On the right hand side $\chi_R(\sigma)$ is the character of $\sigma \in S_n$ in the irreducible representation R of S_n. It may seem strange that R is both a representation of the Symmetric group and Unitary group. Perhaps it even seems strange that this is possible.

This is made possible however by the Frobenius-Schur duality, which relates the representation theory of the symmetric group to the representation theory of the unitary group. The Frobenius-Schur duality arises due to the fact that the actions of $U(N)$ and S_n commute. Commutation together with the fact that there is no degeneracy imply that irreducible representations of $U(N)$ are irreducible representations of S_n (see [38] and references therein). Bear in mind that Young tableaux label the representations of the symmetric group, so R is just some Young tableaux.

On the right hand side one also sees a normalisation factor of $1/n!$ multiplying a sum over the group elements of S_n. $\chi_R(\sigma)$ multiplies the multi-trace over the Z fields. The structure of the multi-trace is determined by the permutation of the indices of the Z fields by the group element σ.

Alternative notation which may be used in defining the Schur polynomials in this dissertation follows:

$$\chi_R(Z) = \frac{1}{n!} \sum_{\sigma \in S_n} \chi_R(\sigma) Tr(\sigma Z^{\otimes n}) \tag{4.2}$$

$Z^{\otimes n}$ should be interpreted as the tensor product of n copies of the matrix Z. $\sigma Z^{\otimes n}$ should then be interpreted as meaning that the group element σ acts on the indices of the tensor product of the Zs, permuting the indices into one another. The trace is needed to ensure that all the indices are contracted.

The two-point function of Schur polynomials in the free field limit is given by (see [8] for proof):

$$\langle \chi_R(Z(x_1)) \chi_S(Z^\dagger(x_2)\rangle = \delta_{RS} \frac{f_R}{(x_1 - x_2)^{2n}} \tag{4.3}$$

The delta function δ_{RS} sets the correlation equal to zero, unless the representation labelled by R is the same as the representation labelled by S. The quantity f_R is the product of the weights[1] of the Young tableaux R and n is the number of matrix fields in each of the Schur polynomials (which is equal to the number of boxes in the Young tableaux labelling the Schur polynomial). Generally the dependence of this quantity on the spacetime co-ordinates (x_1 and x_2) will be suppressed, as the dependence on the spacetime co-ordinates is easily determined by the conformal invariance.

[1] the weight of a box in row i and column j is given by $N - i + j$

Restricted Schur polynomials, are defined as follows (in the case that the Restricted Schur polynomials are comprised of only two types of matrices):

$$\chi_{R(r_1,r_2)}(Z,Y) = \frac{1}{n!m!} \sum_{\sigma \in S_{n+m}} Tr_{(r_1,r_2)}(\Gamma_R(\sigma)) Tr(\sigma Z^{\otimes n} Y^{\otimes m}) \tag{4.4}$$

Here R labels an irreducible representation of S_{n+m} where R is a Young tableaux consisting of $n+m$ boxes. The n Z matrices are organised according to r_1, a Young tableaux consisting of n boxes labelling an irreducible representation of S_n. The m Y matrices are organised by r_2, a Young tableaux consisting of m boxes labelling an irreducible representation of S_m. (r_1, r_2) provides an irreducible representation of $S_n \otimes S_m$. $Tr_{(r_1,r_2)}$ is a restricted trace. This means that the trace is not to be carried out over the carrier space of R, but rather over the subspace of the carrier space of R which can be identified as the carrier space of (r_1, r_2). This is possible because the Young tableaux (r_1, r_2) can be subduced from the Young tableaux R, so there will be a subspace of the carrier space of R which can be identified as the carrier space of (r_1, r_2).

Consider the following example where $R = \yng(2,2)$, and $(r_1, r_2) = (\yng(1,1), \yng(1,1))$. The basis for R is as follows:

$$|\,\young(43,21)\,\rangle = |1\rangle \qquad\qquad |\,\young(42,31)\,\rangle = |2\rangle$$

Clearly $(\yng(1,1), \yng(1,1))$ can only be subduced from $|2\rangle$, thus for this example one finds $Tr_{(r_1,r_2)}(\Gamma_R(\sigma)) = \langle 2|\Gamma_R(\sigma)|2\rangle$. Using the representations of the group elements as given in Appendix D, and equation (4.4), it becomes apparent that the restricted Schur polynomial $\chi_{R(r_1,r_2)}(Z,Y)$ for this example is:

$$\begin{aligned}\chi_{\yng(2,2)\,(\yng(1,1),\yng(1,1))}(Z,Y) = \frac{1}{2}\big[&Tr(Y)^2Tr(Z)^2 + Tr(YZ)^2 + Tr(YZYZ) + Tr(Y)Tr(Z)Tr(YZ) \\ &+ Tr(Y^2Z^2) - Tr(Y^2Z)Tr(Z) - Tr(Y)Tr(YZ^2) - \frac{1}{2}Tr(Y)^2Tr(Z^2) \\ &- \frac{1}{2}Tr(Y^2)Tr(Z)^2\big]\end{aligned}$$

The two point correlator of restricted Schur polynomials is diagonal in the free field theory limit, as is proved in [10]:

$$\langle \chi_{R,(r,s)}(Z,Y) \chi^{\dagger}_{T,(t,u)}(Z,Y) \rangle = \delta_{RT}\delta_{rt}\delta_{su} \frac{(hooks)_R}{(hooks)_r (hooks)_s} f_R. \tag{4.5}$$

"$(hooks)_R$" refers to the product of the hooks of the Young tableaux R. The hooks of the Young tableaux are found by drawing right angled elbows through each block in the Young tableaux. The number of blocks the lines of the elbow pass through gives the hook associated with the block in which the apex of the elbow lies. An example of the construction of the elbows, and the hooks of the Young diagram is shown below.

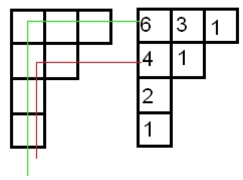

Figure 4.1: Determining the hooks of a Young tableaux

In general the restricted Schur polynomials can be comprised of more than two types of matrices, in this case the above definition is easily generalised. For example:

$$\chi_{R(r_1,r_2,r_3)}(Z,Y,X) = \frac{1}{n!m!l!} \sum_{\sigma \in S_{n+m+l}} Tr_{(r_1,r_2,r_3)}(\Gamma_R(\sigma)) Tr(\sigma Z^{\otimes n} Y^{\otimes m} X^{\otimes l}) \tag{4.6}$$

defines the restricted Schur polynomial consisting of three types of matrices. $Tr_{(r_1,r_2,r_3)}$ is a restricted trace, indicating that the trace must be taken over the subspace of the carrier space of R which can be identified as the carrier space of (r_1, r_2, r_3). Here (r_1, r_2, r_3) is an irreducible representation of $S_n \otimes S_m \otimes S_l$.

It is important to note that Schur polynomials, and their generalisation the restricted Schur polynomials form a complete basis. Due to the fact that the Schur polynomials and restricted Schur polynomials form a complete basis, a product of two Schur polynomials/restricted Schur polynomials can be written as a linear combination of a number of Schur polynomials/Restricted Schur polynomials. In addition to the aforementioned properties, the Schur polynomials and restricted Schur polynomials exhibit other useful properties, which are discussed in [8, 10, 11, 13, 17] to which the reader is referred.

4.2 AdS/CFT interpretation of Schur polynomials

The Schur polynomials and the restricted Schur polynomials are uniquely labelled by the Young tableaux associated with them. Here the correspondence between Schur polynomials and their duals in type IIB string theory is discussed. For a detailed discussion of the correspondence between Young tableaux as labels of Schur polynomials (in $\mathcal{N} = 4$ SYM) and their duals in type IIB string theory see [39].

The simplest Young diagrams, consisting of only a few blocks (i.e. possessing small R-charge) are dual to Kaluza-Klein gravitons on the $AdS_5 \times S^5$ background (see [39]), however this case is not of particular interest in this dissertation and will not be further discussed.

As stated, in [8] it was proposed that certain classes of Schur polynomial were dual to sphere giants and AdS giants respectively. Young diagrams with a large number of boxes in a single column are dual to sphere giant gravitons. The number of rows of a Young diagram is limited to N where N is the dimension of the matrix fields composing the Schur polynomial.

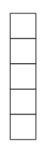 is dual to a sphere giant (4.7)

The limit on the number of boxes that can appear in a column can be understood in terms of the representation theory of $SU(N)$ tensors. In representation theory each box of a Young diagram can be considered an index for a tensor. Vertically stacked boxes in a Young tableaux indicate the tensor is anti-symmetric in the indices represented by the stacked boxes. Horizontally stacked boxes indicate the tensor is symmetric in the indices represented by the stacked boxes. A general Young tableaux consists of horizontally stacked and vertically stacked boxes. In this case the tensor is first to be symmetrised in the indices which are represented by boxes in the same row of the Young tableaux and then anti-symmetrised in the indices represented by the boxes stacked in the same column. The representation theory cut off on the number of boxes in a column is now understood as follows: Given a matrix field of rank N, anti-symmetrising the indices of the tensor product more than N times will result in null tensor hence the number of boxes one is able to stack in a given column is limited (to a maximum of N) by this.

The R-charge of the Schur polynomial is associated with the number of boxes in the Young tableaux labelling the Schur polynomial as each box is associated with the matrix field Z and each Z has 1 unit of R-charge. Further the R-charge of operators in $\mathcal{N} = 4$ SYM is mapped to the angular momentum of their duals in IIB string theory. Recall that sphere giants have a momentum cut off of N units of angular momentum. In this light the fact that the Schur polynomials labelled by completely anti-symmetric Young tableaux are dual to giant gravitons seems plausible.

Duals for the fully symmetric Schur polynomials (i.e. where all the boxes of the Young tableaux are in the same row) were also proposed in [8]. From the representation theory argument above, it can be seen that there is no cut off on angular momentum for the fully symmetric representation. The number of boxes of the fully symmetric Young tableaux can only increase in units of 1. This mirrors the angular momentum for the AdS giants, where flux quantisation forces n (here $n = L$ for stable solutions, see [33] for a discussion on this point) to be integer. This, together with the fact that there is no cut off in angular momentum for an AdS giant, suggests that the fully symmetric Young tableaux is dual to an AdS giant. Explicitly:

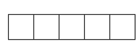 is dual to an AdS giant. (4.8)

Young diagrams of the form:

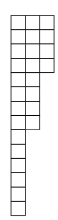

can be interpreted then as three interacting sphere giants at the origin of AdS space. The three giants have different radii in the compact spherical component of $AdS \times S$ and form a three giant system. Similarly the Young diagram corresponding to:

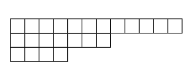

can be interpreted as three interacting AdS giants spreading out to differing extents in the AdS space, forming some kind of three AdS giant system.

This would suggest a naive interpretation that for an operator represented by a Young tableaux,the horizontally stacked boxes represent the extent of the operator's dual in the AdS_5 space, whilst the vertically stacked boxes of the tableaux represent the extent of the operator's dual in the S^5 space.

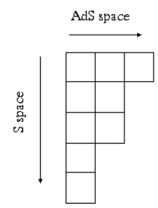

Figure 4.2: Naive AdS/CFT interpretation of directions on Young tableaux

This interpretation is naive however, because as the number of boxes in the Young tableaux grow, so does the energy of the dual to the operator represented by the Young tableaux. When there are $\mathcal{O}(N^2)$ operators in the Young tableaux, the energy of the dual to the operator becomes large enough to deform the geometry via back-reaction. Hence, operators with $\mathcal{O}(N^2)$ boxes are dual to new geometries (see [39], [40],[41] for a detailed discussion on this point).

Part II

Results

Layout:

The order the results are presented in, follows the order in which the research was carried out, as this represents a logical flow connecting the central ideas. The layout for this section follows:

- The action of the Dilatation operator on the basis states of the problem is examined. In doing so a simplification is found which is used for the rest of this dissertation.
- The states under investigation are to be clearly defined. This allows for an investigation of the projectors $P_{R\to(r,s)}$ and $P_{T\to(t,u)}$ which arise naturally in the formula found for the dilatation operator .
- A brief review of the results found in [18] is given.
- The results of the calculation in the case of three impurities is given.
- The results of the calculation in the case of four impurities is given.
- The results are analysed and the conclusions reached discussed.

Chapter 5

New formula for the dilatation operator

Recall that in the $SU(2)$ sector the dilatation operator and the one loop piece thereof are given by:

$$\mathcal{D} = \sum_{j=0}^{\infty} (\frac{g_{YM}^2}{16\pi^2})^j \mathcal{D}_{2j}$$

Where

$$\mathcal{D}_0 = Tr\big(Y\frac{d}{dY}\big) + Tr\big(Z\frac{d}{dZ}\big) \tag{5.1}$$

$$\mathcal{D}_2 = -Tr\big([Y,Z][\frac{d}{dY},\frac{d}{dZ}]\big) \tag{5.2}$$

Note: In this dissertation $g_{YM}^2\mathcal{D}_2$ is of primary interest. For notational ease $g_{YM}^2\mathcal{D}_2$ will be written as $\mathcal{D}$. From this point onwards reference to the dilatation operator will refer to the one loop contribution (previously $g_{YM}^2\mathcal{D}_2$, but now written as $\mathcal{D}$) which calculates the anomalous dimension in units of energy. The full dilatation operator (tree level contribution plus corrections) will always be referred to as the full dilatation operator, to avoid confusion.

The one loop contribution to the anomalous dimension is to be calculated for restricted Schur polynomial operators built out of the two matrices Z and Y (as discussed in Chapter 3). Therefore the calculation to be carried out is:

$$-g_{YM}^2 Tr\big([Z,Y][\frac{d}{dZ},\frac{d}{dY}]\big)\chi_{R,(r,s)}(Z,Y)$$

Notice that by definition of the dilatation operator the Z matrices and the Y matrices are treated equally. Hence:

$$
\begin{aligned}
&\mathcal{D}\chi_{R,(r,s)}(Z,Y) \\
&= -[Z,Y]^j{}_k[\frac{d}{dZ},\frac{d}{dY}]^k{}_j\frac{g_{YM}^2}{n!m!}\sum_{\sigma\in S_{n+m}} Tr_{(r,s)}(\Gamma_R(\sigma))Z^{i_1}_{i_{\sigma(1)}}\cdots Z^{i_n}_{i_{\sigma(n)}}Y^{i_{n+1}}_{i_{\sigma(n+1)}}\cdots Y^{i_{n+m}}_{i_{\sigma(n+m)}} \\
&= \frac{g_{YM}^2}{(n-1)!(m-1)!}\sum_{\sigma\in S_{n+m}} Tr_{(r,s)}(\Gamma_R(\sigma))Z^{i_1}_{i_{\sigma(1)}}\cdots Z^{i_{n-1}}_{i_{\sigma(n-1)}}Y^{i_{n+2}}_{i_{\sigma(n+2)}}\cdots Y^{i_{n+m}}_{i_{\sigma(n+m)}}\times \\
&\times [Z,Y]^j{}_k(\delta^{i_n}_j\delta^l_{i_{\sigma(n)}}\delta^{i_{n+1}}_l\delta^k_{i_{\sigma(n+1)}}-\delta^{i_{n+1}}_j\delta^l_{i_{\sigma(n+1)}}\delta^{i_n}_l\delta^k_{i_{\sigma(n)}}) \\
&= \frac{g_{YM}^2}{(n-1)!(m-1)!}\sum_{\sigma\in S_{n+m}} Tr_{(r,s)}(\Gamma_R(\sigma))Z^{i_1}_{i_{\sigma(1)}}\cdots Z^{i_{n-1}}_{i_{\sigma(n-1)}}Y^{i_{n+2}}_{i_{\sigma(n+2)}}\cdots Y^{i_{n+m}}_{i_{\sigma(n+m)}}\times \\
&\times \left([Z,Y]^{i_n}_{i_{\sigma(n+1)}}\delta^{i_{n+1}}_{i_{\sigma(n)}}-[Z,Y]^{i_{n+1}}_{i_{\sigma(n)}}\delta^{i_n}_{i_{\sigma(n+1)}}\right)
\end{aligned}
$$

Note that the second term is very similar to the first, to exploit this relabel $(n \leftrightarrow n+1)$ in the second term. This is done by conjugating σ by $(n,n+1)$ (a transposition in S_{n+m}) to get:

$$
\begin{aligned}
&= \frac{g_{YM}^2}{(n-1)!(m-1)!}\sum_{\sigma\in S_{n+m}} Tr_{(r,s)}(\Gamma_R(\sigma-(n,n+1)\sigma(n,n+1))) \\
&Z^{i_1}_{i_{\sigma(1)}}\cdots Z^{i_{n-1}}_{i_{\sigma(n-1)}}Y^{i_{n+2}}_{i_{\sigma(n+2)}}\cdots Y^{i_{n+m}}_{i_{\sigma(n+m)}}[Z,Y]^{i_n}_{i_{\sigma(n+1)}}\delta^{i_{n+1}}_{i_{\sigma(n)}}
\end{aligned}
$$

Change the variable of summation to $\psi=\sigma(n,n+1)$.

$$
\begin{aligned}
&= \frac{g_{YM}^2}{(n-1)!(m-1)!}\sum_{\psi\in S_{n+m}} Tr_{(r,s)}(\Gamma_R(\psi(n,n+1)-(n,n+1)\psi)) \\
&Z^{i_1}_{i_{\psi(1)}}\cdots Z^{i_{n-1}}_{i_{\psi(n-1)}}Y^{i_{n+2}}_{i_{\psi(n+2)}}\cdots Y^{i_{n+m}}_{i_{\psi(n+m)}}[Z,Y]^{i_n}_{i_{\psi(n)}}\delta^{i_{n+1}}_{i_{\psi(n+1)}}
\end{aligned}
$$

A coset expansion is used to eliminate the delta function. The dimension of the matrices is N so, $\delta^{i_{n+1}}_{i_{n+1}}=N$. Performing a coset expansion on a function $f(\psi)$ one gets:

$$
\begin{aligned}
&\sum_{\psi\in S_{n+m}} f(\psi) = \sum_{\psi\in S_{n+m-1}}\sum_{i=1}^{n+m} f(\psi(i,n+1)) \\
&\Rightarrow \mathcal{D}\chi_{R,(r,s)}(Z,Y) \\
&= \frac{g_{YM}^2}{(n-1)!(m-1)!}\sum_{\psi\in S_{n+m-1}} Tr_{(r,s)}\Big(\Gamma_R\big([\psi,(n,n+1)](N+\sum_{\substack{i=1\\ i\neq n+1}}^{n+m}(i,n+1))\big)\Big) \\
&Z^{i_1}_{i_{\psi(1)}}\cdots Z^{i_{n-1}}_{i_{\psi(n-1)}}Y^{i_{n+2}}_{i_{\psi(n+2)}}\cdots Y^{i_{n+m}}_{i_{\psi(n+m)}}[Z,Y]^{i_n}_{i_{\psi(n)}}
\end{aligned}
$$

Here S_{n+m-1} is the subgroup of S_{n+m} which leaves $n+1$ invariant, explicitly $\psi(n+1) = n+1$ for all ψ in S_{n+m-1}. The box carrying the label $n+1$ is correctly interpreted as the box removed to subduce a representation R' from representation R. As $\psi \in S_{n+m-1} \subseteq S_{n+m}$, and R does not provide an irreducible representation of S_{n+m-1}, $\Gamma_R(\psi)$ must be reducible. In particular, it must then be possible to write $\Gamma_R(\psi)$ as $\oplus_{R'}\Gamma_{R'}(\psi)$. Here the direct sum runs over all possible irreducible representations R' of S_{n+m-1} which can be subduced from R (this point is also briefly discussed in Appendix C).

Given a subduced representation R',

$$N + \sum_{\substack{i=1 \\ i \neq n+1}}^{n+m} (i, n+1) = c_{RR'}.$$

Here $c_{RR'}$ is the weight of the box removed to subduce R' from R. In the following the sum over R' runs over all possible representations R' which can be subduced from R.

$$\Rightarrow \mathcal{D}\chi_{R,(r,s)}(Z,Y)$$

$$= \frac{g_{YM}^2}{(n-1)!(m-1)!} \sum_{\psi \in S_{n+m-1}} \sum_{R'} c_{RR'} Tr_{(r,s)}\Big(\Gamma_{R'}(\psi)\Gamma_R((n,n+1)) - \Gamma_R((n,n+1))\Gamma_{R'}(\psi)\Big)$$

$$Z^{i_1}_{i_{\psi(1)}} \cdots Z^{i_{n-1}}_{i_{\psi(n-1)}} Y^{i_{n+2}}_{i_{\psi(n+2)}} \cdots Y^{i_{n+m}}_{i_{\psi(n+m)}} [Z,Y]^{i_n}_{i_{\psi(n)}}$$

Using the notation explained in Chapter 4. One may write:

$$Z^{i_1}_{i_{\psi(1)}} \cdots Z^{i_{n-1}}_{i_{\psi(n-1)}} Y^{i_{n+2}}_{i_{\psi(n+2)}} \cdots Y^{i_{n+m}}_{i_{\psi(n+m)}} (ZY-YZ)^{i_n}_{i_{\psi(n)}} = Tr\Big(\big(\psi(n,n+1)-(n,n+1)\psi\big)Z^{\otimes n}Y^{\otimes m}\Big)$$

In [17] it was shown that:

$$Tr(\sigma Z^{\otimes n} Y^{\otimes m}) = \sum_{T,(t,u)} \frac{d_T n! m!}{dtdu(n+m)!} \chi_{T,(t,u)}(\sigma^{-1}) \chi_{T,(t,u)}(Z,Y)$$

Here d_T is the dimension of irreducible representation (irrep) T, d_t the dimension of irrep t and d_s the dimension of irrep s. Thus:

$$\mathcal{D}\chi_{R,(r,s)}(Z,Y) = \sum_{T,(t,u)} M_{R,(r,s);T,(t,u)} \chi_{T,(t,u)}(Z,Y)$$

where

$$M_{R,(r,s);T,(t,u)} = \sum_{\psi \in S_{n+m-1}} \sum_{R'} \frac{c_{RR'} d_T nm}{d_t d_u (n+m)!} Tr_{(r,s)}\Big(\Gamma_{R'}(\psi)\Gamma_R((n,n+1)) - \Gamma_R((n,n+1))\Gamma_{R'}(\psi)\Big) \times$$

$$\times \chi_{T,(t,u)}((n,n+1)\psi^{-1} - \psi^{-1}(n,n+1)) g_{YM}^2$$

In the same way representations R' were subduced from R, representations T' may be subduced from T to give:

$$
\begin{aligned}
M_{R,(r,s);T,(t,u)} = & \sum_{\psi \in S_{n+m-1}} \sum_{R',T'} \frac{c_{RR'} d_T nm}{d_t d_u (n+m)!} \times \\
& \times Tr_{(r,s)} \Big(\Gamma_{R'}(\psi) \Gamma_R((n,n+1)) - \Gamma_R((n,n+1)) \Gamma_{R'}(\psi) \Big) \times \\
& \times Tr_{(t,u)} \Big(\Gamma_T((n,n+1)) \Gamma_{T'}(\psi^{-1}) - \Gamma_{T'}(\psi^{-1}) \Gamma_T((n,n+1)) \Big) g_{YM}^2
\end{aligned}
$$

Note that $Tr_{(r,s)}(\sigma) = Tr(P_{R\to(r,s)}\sigma)$, where $P_{R\to(r,s)}$ is a projector projecting from the carrier space of R to the carrier space of (r,s) . This allows one to write:

$$
\begin{aligned}
& = g_{YM}^2 \sum_{\psi \in S_{n+m-1}} \sum_{R',T'} \frac{c_{RR'} d_T nm}{d_t d_u (n+m)!} \times \\
& \times Tr\Big(P_{R\to(r,s)} \big(\Gamma_{R'}(\psi) \Gamma_R((n,n+1)) - \Gamma_R((n,n+1)) \Gamma_{R'}(\psi) \big) \Big) \times \\
& \times Tr\Big(P_{T\to(t,u)} \big(\Gamma_T((n,n+1)) \Gamma_{T'}(\psi^{-1}) - \Gamma_{T'}(\psi^{-1}) \Gamma_T((n,n+1)) \big) \Big)
\end{aligned} \tag{5.3}
$$

After multiplying out the above and writing everything in index notation,the fundamental orthogonality theorem (B.1) is easy to apply. The result after application is:

$$
\mathcal{D}\chi_{R,(r,s)}(Z,Y) = \sum_{T,(t,u)} M_{R,(r,s);T,(t,u)} \chi_{T,(t,u)}(Z,Y) \tag{5.4}
$$

where

$$
\begin{aligned}
& M_{R,(r,s);T,(t,u)} = g_{YM}^2 \sum_{R'} \frac{c_{RR'} d_T nm}{d_{R'} d_t d_u (n+m)} \times \\
& \times Tr\Big([P_{R\to(r,s)}, \Gamma_R((n,n+1))] I_{R'T'} [\Gamma_T((n,n+1)), P_{T\to(t,u)}] I_{T'R'} \Big)
\end{aligned} \tag{5.5}
$$

The objects $I_{R'T'}$ are called intertwiners (for a discussion of the intertwiners and how they arise in the last steps see Appendix C), the purpose of the intertwiners is to glue the R' subspace to the T' subspace. The above gives a computationally easier form of the action of the dilatation operator on the basis of restricted Schur polynomials formed from two types of matrices. The above formula then represents an important result of the research carried out.

In the above proof it is important to note that the fundamental orthogonality theorem results in a term of $\delta_{R'T'}$, which is summed over to result in the intertwiners. Thus the R' and T' subspaces must be equivalent, which in turn means that R and T can differ by at most a placement of a single box. The operator mixing is therefore constrained in that the operators which mix can differ by at most moving a single box around on the Young tableaux labelling the operators (a similar result was found in [12, 13] where open strings take the place of the impurities studied here). The fact that these systems can differ by at most the placement of a single box on their Young tableaux points to locality in the action of the dilatation operator. Thus only two giant systems which are similar (in that the Young tableaux labelling the systems are similar) mix under the action of the dilatation operator.

For the spectrum of the anomalous dimensions, the action of the dilatation operator must be computed for normalised operators. The normalised operators $O_{R,(r,s)}$ are defined so that:

$$\chi_{R,(r,s)}(Z,Y) = \sqrt{f_R \frac{(hooks)_R}{(hooks)_r (hooks)_s}} O_{R,(r,s)}$$

Substituting into (4.5) it is easy to see that the operators $O_{R,(r,s)}$ are correctly normalised as:

$$\langle O_{R,(r,s)}(Z,Y) O^\dagger_{T,(t,u)}(Z,Y) \rangle = \delta_{RT}\delta_{rt}\delta_{su}$$

Substituting the normalised operators into (5.4) gives:

$$\mathcal{D} O_{R,(r,s)}(Z,Y) = \sum_{T,(t,u)} N_{R,(r,s);T,(t,u)} O_{T,(t,u)}(Z,Y) \tag{5.6}$$

where

$$N_{R,(r,s);T,(t,u)} = g_{YM}^2 \sum_{R'} \frac{c_{RR'} d_T nm}{d_{R'} d_t d_u (n+m)} \sqrt{\frac{f_T (hooks)_T (hooks)_r (hooks)_s}{f_R (hooks)_R (hooks)_t (hooks)_u}} \times$$
$$\times\, Tr\Big([P_{R\to(r,s)}, \Gamma_R((n,n+1))] I_{R'T'} [\Gamma_T((n,n+1)), P_{T\to(t,u)}] I_{T'R'} \Big)$$

The above expression was used for the evaluation of the dilatation operator on the class of restricted Schur polynomials containing three impurities and four impurities. The results of the calculation will be presented in the remaining part of this thesis.

5.1 Excited Giant Graviton Bound States

The following extends upon the AdS/CFT interpretation of Schur polynomials (as discussed in Chapter 4.2) to include restricted Schur polynomials. In doing so, the operators under investigation are clearly defined.

Following Chapter 4.2, a Schur polynomial labelled by a Young tableaux with two columns can be interpreted as a bound state of two giant gravitons. The restricted Schur polynomials under investigation are different in that they are formed from two types of matrices. The Young tableaux labelling restricted Schur polynomials are expected to be of the form:

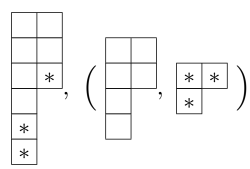

The $*$'s represent impurities, blocks in the Young tableaux which represent the matrix Y rather than Z. Removing the impurities from the irrep R produces the irrep r. The impurities are organised into irrep s. This looks very much like a system of two bound giant gravitons, excepting that there are impurities present. The impurities correspond to excitations in the system of two giant gravitons. In the case that the two columns of the Young tableaux are vastly separated (i.e. the longer column is $\mathcal{O}\sqrt{N}$ boxes longer than the shorter column), the excitations can be thought as being localized on the giant graviton represented by the column on which the impurity lies.

In this dissertation the number of impurities is set to $\mathcal{O}(1)$. This is not because of a shortcoming of the calculation method used, as in principle there is no problem with performing the calculation for $\mathcal{O}(N)$ impurities, but because the complexity of the calculation increases as impurities are added. The difference between the number of boxes in the two columns is measured by the parameter a, where a was limited to the value a_{max} for the numerical calculation of the spectrum of anomalous dimensions. The difference in the length of the two columns is small in comparison to the length of the shorter column. The number of Z's appearing is αN where $2 - \alpha = \zeta \ll 1$. To understand this limit consider the following:

It can be seen that the number of Zs is given by $n(Z) = 2N - a_{max} - n(Y)$

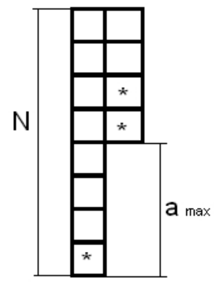

Figure 5.1: General operator of interest

where $n(Z)$ is the number of Zs and $n(Y)$ is the number of Ys. Then, as $n(Z)$ is of $\mathcal{O}(N)$, it can be seen that: $n(Z) = \alpha N = 2N - a_{max} - n(Y)$ which implies that $N(2-\alpha) = a_{max} + n(Y)$. Dividing this by N and dropping $n(Y)/N$ (this is justified as $n(Y) \sim \mathcal{O}(1)$) gives $2 - \alpha = \zeta \ll 1$, where $a_{max}/N = \zeta$.

It proves convenient to introduce two other parameters in the calculation, namely b_0 and b_1. b_0 is defined as the number of rows with two boxes in representation r and b_1 is defined as the number of rows with 1 box in representation r. From the above arguments it is clear that in the large N limit, b_0 is of $\mathcal{O}(N)$. Further, by considering the normalisation factor $\sqrt{\frac{f_T (hooks)_T (hooks)_r (hooks)_s}{f_R (hooks)_R (hooks)_t (hooks)_u}}$ given b_0 is $\mathcal{O}(N)$, it can be seen that restricted Schur polynomials with an impurity in the third column are suppressed by a factor of $\mathcal{O}(1/\sqrt{N})$.

The parameters b_0 and b_1 are not independent. To see this let the total number of boxes in the Young tableaux be M, let the representation theory limit on the number of boxes in a single column be N, let the number of impurities be I and let b_0, b_1 and a_{max} be defined as above. Then it can be seen that:

$$\begin{aligned} 2b_0 + b_1 + I &= M \\ 2N - a_{max} &= M \\ \Rightarrow b_0 &= N - \frac{I + a_{max} + b_1}{2} \end{aligned}$$

To dispel any possible doubts about the definition of b_0 and b_1, an example is given below:

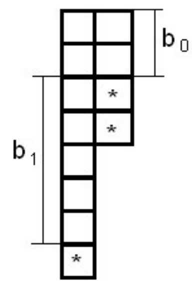

Figure 5.2: Diagram showing definition of b_0 and b_1

The diagram shown above is the diagram corresponding to the irreducible representation R of S_{12}. The boxes containing the $*$s are to be removed to obtain the irreducible representation r of S_9.

Chapter 6

The projection operators

The operators $P_{R\to(r,s)}$ and $P_{T\to(t,u)}$ arise in the formula for the Dilatation operator. The projector $P_{R\to(r,s)}$ projects from the representation R of S_{n+m} to (r,s) which is an irreducible representation of $S_n \times S_m$. The operators labelled by Young tableaux consisting of two columns do not mix with operators labelled by Young tableaux with a differing number of columns, thus the projectors defined need only work on operators associated with Young tableaux consisting of two columns. This simplifies the problem considerably.

In general (r,s) may be subduced from R more than once. Thus specifying R, r and s does not uniquely identify how (r,s) was subduced from R. An example of this multiplicity problem is given below, where (r,s) may can be subduced twice from R. Consider the representation R, as before, the boxes containing $*$s represent impurities. Removing the impurities from R leaves the representation r. Note that as the boxes representing impurities have no edges in common, any organisation of the removed boxes is possible.

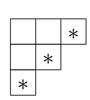

r is uniquely determined, so one can focus entirely on the possible s. The possible irreducible representations s which may be subduced can be related to the tensor product (in $SU(N)$ representation theory) of the three removed impurities. This is a consequence of the Frobenius-Schur duality, which relates the representation theory of the unitary group to that of the symmetric group.

Hence to find the possible subduced irreps s consider the following:

$$
\begin{aligned}
\ydiagram{1} \otimes \left(\ydiagram{1} \otimes \ydiagram{1} \right) &= \left(\ydiagram{1} \otimes \ydiagram{2} \right) \oplus \left(\ydiagram{1} \otimes \ydiagram{1,1} \right) \\
&= \left(\ydiagram{3} \oplus \ydiagram{2,1} \right) \oplus \left(\ydiagram{2,1} \oplus \ydiagram{1,1,1} \right).
\end{aligned}
$$

As seen, given the three blocks which can be pulled off R, the representation $(\ydiagram{2,1}, \ydiagram{2,1})$ can be subduced twice. Thus in the three column case the multiplicity means the projector $P_{\ydiagram{3,2,1} \to (\ydiagram{2,1}\,,\, \ydiagram{2,1})}$ is not uniquely defined. In general it is difficult to identify a concrete condition with which to choose a definite projector.

When the Young tableaux have only two columns there is no multiplicity problem as there is only one way of subducing (r, s) from R. Thus the problem simplifies considerably. Bearing this in mind, one can see that given R and the boxes to be removed to obtain r, every representation can be subduced only once. Recall that the symmetries of adjacent edges of the Young tableaux must be preserved. The following gives an example of how the possible subductions (r, s) of R can be identified, given the boxes to be removed:

$$
\begin{ytableau}
\, & \, \\
\, & \, \\
\, & * \\
\, & * \\
\, \\
\, \\
\, \\
*
\end{ytableau}
$$

The two possible subduced representations are:

$$
\ydiagram{2,2,1,1,1,1,1} \quad \ydiagram{1,1,1} \qquad\qquad \ydiagram{2,2,1,1,1,1,1} \quad \ydiagram{2,1}
$$

Given the above representation of S_{12}, all possible of subductions $S_9 \times S_3$ can be subduced, and the subductions are unique. To check this one can simply note that the dimension of the above representation of S_{12} is 275. The irreducible representations:

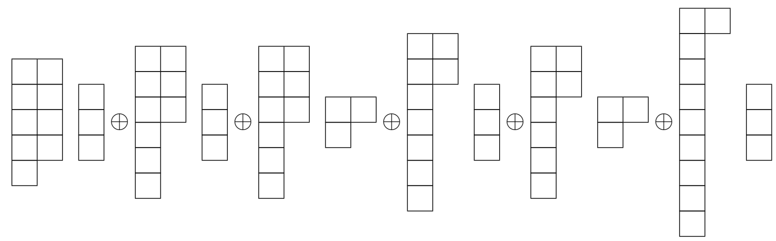

Have dimension 42, 48, 96, 27, 54, and 8 which sum to give 275, the dimension of R.

From the above discussion, it can be seen that given R, the boxes removed to get r and the irreducible representation s, the projector is uniquely defined. In this case the projector is easily defined, as there is no multiplicity problem. The projector [1]:

$$P_s = \frac{d_s}{m!} \sum_{\sigma \in S_m} \chi_s(\sigma)\Gamma_R(\sigma) \tag{6.1}$$

correctly organises the removed boxes to reproduce s. Further, the boxes which must be removed from R to get r are also of importance, this is encoded into the above projector by allowing it to only act on a certain subspace. The projector acts on the subspace in which the boxes which must be removed to get r from R are labelled as such. As an example, consider the following representation R where the boxes to be removed to get r contain a $*$.

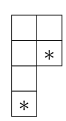

The projector will act on the six dimensional subspace (recall d 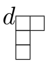 $= 3$) spanned by the two sets of states:

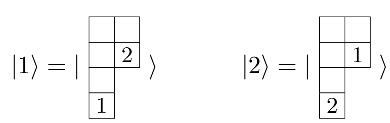

The basis used throughout is the well known Young-Yamonouchi basis.

[1]It will be proved that (6.1) is a projector in Appendix B

Chapter 7

Results from the Dilatation operator

The action of the dilatation operator on three and four impurity states was calculated, however the results are rather cumbersome, so will be left for Appendix A. The dilatation operator was numerically diagonalised to determine the anomalous dimensions for two column restricted Schur polynomials with three and four impurities ($I = 3, 4$). The calculation was carried out as follows:

- For an arbitrary value of a, where $I < a < a_{max} - 2$ the generators of S_m were calculated (by hand) in the representations R, T, s and u. These generators were then used together with a computer algebra program (Mathematica 7) to calculate all the group elements of S_m in representations R, T, s and u. Using the results together with equation (6.1) the projection operators were defined and saved to disk.

- $\Gamma_R((n, n+1))$ and $\Gamma_T((n, n+1))$ were calculated (by hand) and saved. This allowed for the computation of the commutators $[P_{R\to(r,s)}, \Gamma_R((n, n+1))]$ and $[\Gamma_T((n, n+1)), P_{T\to(t,u)}]$, and hence the evaluation of the dilatation operator to be carried out according equation (5.6).

- The above procedure was carried out for all possible values of a where $I < a < a_{max} - 2$ (by computer).

- For $a \leq I$ or $a \geq a_{max} - 2$ care was taken not to include mixing between legitimate operators (where $0 \leq a \leq a_{max}$) and illegitimate operators (where $a < 0$ or $a > a_{max}$), and consequently this was done by hand.

- All the possible operators were then systematically labelled, which allows one to write equation (5.6) as a matrix equation, in which the action of the dilatation operator on the various restricted Schur polynomials is encoded by the matrix entries.

- This matrix was then diagonalised (by computer) for randomly chosen values of a_{max} and the spectra were analysed.

A simplifying limit was investigated where the action of the dilatation operator appears to be that of a lattice second derivative (this occurs when the longer column of the Young tableaux has $\mathcal{O}(\sqrt{N})$ more boxes than the shorter column). The Young tableaux plays the role of the lattice in this case. Here the numerical spectra obtained are given as well as the action of the dilatation operator in the aforementioned simplifying limit for the cases where the operators have three and four impurities. A review of the results found in [18] for the case where the operators have two impurities is also given.

Finally, note that the parameter a_{max} (and by extension all a's) was assumed to be even. In the case that $a_{max} \to \infty$ (which is the case of interest) one cannot differentiate whether a_{max} is odd or even, so the assumption that a_{max} is even does not affect the generality of the result.

7.1 The two impurity case

This section reviews the results found in [18]. These operators are built using two impurities (Ys) and many Zs. In the case of two impurities s is a representation of S_2, r is a representation of S_n and R is a representation of S_{n+2}. As discussed in Chapter 5.1 the parameter b_0 is of size $\mathcal{O}(N)$ and the parameter b_1 ranges from 0 to a_{max} of size $\mathcal{O}(N)$. The operators which can be defined follow:

$\chi_A(b_0, b_1) = \chi$ 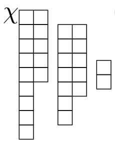 (Z, Y)

$\chi_B(b_0, b_1) = \chi$ 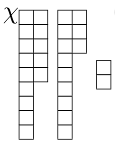 (Z, Y)

$\chi_D(b_0, b_1) = \chi$ 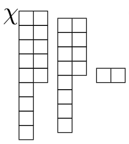 (Z, Y)

$\chi_E(b_0, b_1) = \chi$ 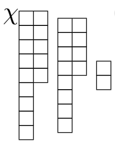 (Z, Y)

7.1.1 Spectrum

If both the columns have the same length ($a = 0$), then of the above operators only operator χ_B and χ_D are defined. For $a = 2$ to $a = a_{max}$ all four states are defined. Hence given a value of a_{max} there are $2 + 4(\frac{a_{max}}{2}) = 2a_{max} + 2$ states. It is found that there are $\frac{3}{2}a_{max} + 1$ zero eigenvalues. The remaining eigenvalues are given by:

$$\lambda_i = 8ig_{YM}^2 \qquad i = 1, 2, \ldots, \frac{1}{2}a_{max} + 1$$

7.1.2 Discretised second derivative

The calculation is carried out in the t'Hooft limit ($g_{YM}^2 N = \lambda$, where λ is some finite constant). The normalised operators (as defined in Chapter 5) are used. In the limit that $N - b_0 = \mathcal{O}(N)$, $b_0 = \mathcal{O}(N)$ and $b_1 = \mathcal{O}(\sqrt{N})$ the dynamics of the one loop dilatation operator simplify. Recall that the length of the columns of the operators are mapped to the angular momentum of their giant graviton duals, and the angular momentum of a giant graviton determines its size. In this limit then the system should be described by two giant gravitons, separated by a distance of $\mathcal{O}(1)$ string units, with open strings stretching between them.

The dynamics are expected to simplify. In this limit the action of the dilatation operator becomes:

$$\mathcal{D}O_A(b_0,b_1) = g_{YM}^2(N-b_0)\times\mathcal{O}(\frac{1}{b_1})$$
$$\mathcal{D}O_B(b_0,b_1) = g_{YM}^2(N-b_0)\times\mathcal{O}(\frac{1}{b_1})$$

$$\begin{aligned}\mathcal{D}O_D(b_0,b_1) =& -g_{YM}^2(N-b_0)[O_D(b_0+1,b_1-2)-2O_D(b_0,b_1)+O_D(b_0-1,b_1+2)]\\&+g_{YM}^2(N-b_0)[O_E(b_0+1,b_1-2)-2O_E(b_0,b_1)+O_E(b_0-1,b_1+2)]\\&+N\times\mathcal{O}(\frac{1}{b_1})\\\mathcal{D}O_E(b_0,b_1) =& -g_{YM}^2(N-b_0)[O_E(b_0+1,b_1-2)-2O_E(b_0,b_1)+O_E(b_0-1,b_1+2)]\\&+g_{YM}^2(N-b_0)[O_D(b_0+1,b_1-2)-2O_D(b_0,b_1)+O_D(b_0-1,b_1+2)]\\&+N\times\mathcal{O}(\frac{1}{b_1})\end{aligned}$$

In the aforementioned limit, the action of the Dilatation operator on the states $O_A(b_0,b_1)$ and $O_B(b_0,b_1)$ give zero eigenvalues of the Dilatation operator and thus they are supersymmetric. $O_A(b_0,b_1)$ and $O_B(b_0,b_1)$ can be interpreted as the states in which only the larger threebrane and smaller threebrane are deformed respectively. In [18, 35] it was shown that the deformations (all the deformations of the type considered in this dissertation) of a single threebrane giant graviton are supersymmetric. Thus it seems natural that $O_A(b_0,b_1)$ and $O_B(b_0,b_1)$ remain supersymmetric. It is also seen that $O_D(b_0,b_1)+O_E(b_0,b_1)$ is supersymmetric, thus making three supersymmetric operators. Note also that the action of $\mathcal{D}$ on the combination $O_D(b_0,b_1) - O_E(b_0,b_1) = O_{D-E}(b_0,b_1)$ gives:

$$\mathcal{D}O_{D-E}(b_0,b_1) = -2g_{YM}^2(N-b_0)[O_{D-E}(b_0+1,b_1-2)-2O_{D-E}(b_0,b_1)+O_{D-E}(b_0-1,b_1+2)]$$

This looks exactly like a lattice discretisation of the second derivative, where the Young tableaux itself defines the lattice. Operator mixing is restricted to cases where the operators which mix are related by the movement of one box of their Young tableaux. Thus the physics is local, as is seen from the appearance of the second derivative.

7.2 Three impurity case

Here the operators are built out of many Zs and three Ys. Again b_0 is of size $\mathcal{O}(N)$ and b_1 ranges from 0 to size $\mathcal{O}(N)$. Here there are six possible operators which can be defined. These follow:

$\chi_A(b_0, b_1) = \chi$ 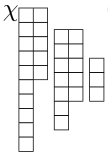 (Z, Y) $\qquad$ $\chi_B(b_0, b_1) = \chi$ 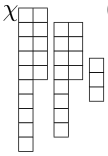 (Z, Y)

$\chi_C(b_0, b_1) = \chi$ 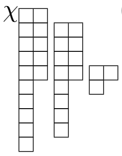 (Z, Y) $\qquad$ $\chi_D(b_0, b_1) = \chi$ 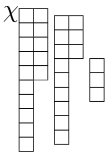 (Z, Y)

$\chi_E(b_0, b_1) = \chi$ 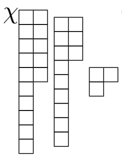 (Z, Y) $\qquad$ $\chi_F(b_0, b_1) = \chi$ 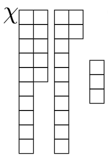 (Z, Y)

7.2.1 Spectrum

When the two columns have the same length, only the operators χ_E and χ_F can be defined. When the longer column is two boxes longer than the shorter column, all the operators excluding χ_A can be defined, thus for $a \leq 2$ there are seven states. For any value of a greater than 2, all six states can be defined, so given some value for $a_{max} > 2$ there are $\frac{6}{2}(a_{max} - 2) + 7 = 3a_{max} + 1$ states in total. Performing the calculation, it is found that there are $2a_{max}$ zero eigenvalues, corresponding to supersymmetric states. Of the $a_{max} + 1$ non-zero eigenvalues, there are $\frac{a_{max}}{2}$ doubly degenerate eigenvalues, given by:

$$\lambda_i = 8ig_{YM}^2 \qquad i = 1, 2, \ldots, \frac{a_{max}}{2}$$

Finally there is a single state with an eigenvalue of $\lambda = 4a_{max} + 8$. The degeneracies in the spectrum (for the non-zero eigenvalues) points to a symmetry enhancement in the large N limit.

7.2.2 Discretised second derivative

In the limit where $N - b_0 = \mathcal{O}(N)$, $b_0 = \mathcal{O}(N)$ and $b_1 = \mathcal{O}(\sqrt{N})$ the dynamics of the system simplify significantly. As before, the calculation is carried out in the t'Hooft limit and the previously defined normalised operators are used. The action of the dilatation operator in this limit is given by:

$$\mathcal{D}O_A(b_0, b_1) = g_{YM}^2 \, (N - b_0) \times O\left(\frac{1}{b_1}\right)$$

$$\begin{aligned}\mathcal{D}O_B(b_0, b_1) =& -\frac{4}{3} g_{YM}^2 \, (N - b_0) \left[O_B(b_0 + 1, b_1 - 2) - 2\, O_B(b_0, b_1) + O_B(b_0 - 1, b_1 + 2)\right] \\ &+ \frac{2\sqrt{2}}{3} g_{YM}^2 \, (N - b_0) \left[O_C(b_0 + 1, b_1 - 2) - 2O_C(b_0 + 1, b_1) + O_C(b_0 - 1, b_1 + 2)\right]\end{aligned}$$

$$\begin{aligned}\mathcal{D}O_C(b_0, b_1) =& \frac{2\sqrt{2}}{3} g_{YM}^2 (N - b_0) \left[O_B(b_0 + 1, b_1 - 2) - 2O_B(b_0, b_1) + O_B(b_0 - 1, b_1 + 2)\right] \\ &- \frac{2}{3} g_{YM}^2 (N - b_0) \left[O_C(b_0 + 1, b_1 - 2) - 2O_C(b_0, b_1) + O_C(b_0 - 1, b_1 + 2)\right]\end{aligned}$$

$$\begin{aligned}\mathcal{D}O_D(b_0, b_1) =& -\frac{4}{3} g_{YM}^2 (N - b_0) \left[O_D(b_0 + 1, b_1 - 2) - 2O_D(b_0, b_1) + O_D(b_0 - 1, b_1 + 2)\right] \\ &+ \frac{2\sqrt{2}}{3} g_{YM}^2 (N - b_0) \left[O_E(b_0 + 1, b_1 - 2) - 2O_E(b_0, b_1) + O_E(b_0 - 1, b_1 + 2)\right]\end{aligned}$$

$$\begin{aligned}\mathcal{D}O_E(b_0, b_1) =& \frac{2\sqrt{2}}{3} g_{YM}^2 (N - b_0) \left[O_D(b_0 + 1, b_1 - 2) - 2O_D(b_0, b_1) + O_D(b_0 - 1, b_1 + 2)\right] \\ &- \frac{2}{3} g_{YM}^2 (N - b_0) \left[O_E(b_0 + 1, b_1 - 2) - 2O_E(b_0, b_1) + O_E(b_0 - 1, b_1 + 2)\right]\end{aligned}$$

$$\mathcal{D}O_F(b_0, b_1) = g_{YM}^2 \, (N - b_0) \times O\left(\frac{1}{b_1}\right)$$

In this limit the operators $O_A(b_0, b_1)$ and $O_F(b_0, b_1)$ are again zero eigenstates of the Dilatation operator and are therefore supersymmetric. $O_A(b_0, b_1)$ is the state in which only the larger threebrane is deformed and $O_F(b_0, b_1)$ is the state in which only the smaller threebrane is deformed. Following the results of [18, 35], the fact that $O_A(b_0, b_1)$ and $O_F(b_0, b_1)$ remain supersymmetric seems natural as only one of the giant gravitons was deformed. It is easy to see that the action of the dilatation operator on $O_B(b_0,b_1)+\sqrt{2}O_C(b_0,b_1)$ and $O_D(b_0,b_1)+\sqrt{2}O_E(b_0,b_1)$ produces zero eigenvalues, these are therefore supersymmetric. In this limit then, there are four supersymmetric ways to deform the system of two giant gravitons. Define $O_B(b_0,b_1)-\frac{1}{\sqrt{2}}O_C(b_0,b_1)=O_{B-C}(b_0,b_1)$ and $O_D(b_0,b_1)-\frac{1}{\sqrt{2}}O_E(b_0,b_1)=O_{D-E}(b_0,b_1)$. The action of the Dilatation operator on the operators $O_{B-C}(b_0,b_1)$ and $O_{D-E}(b_0,b_1)$ gives:

$$
\begin{aligned}
\mathcal{D}O_{B-C}(b_0,b_1) = &\quad -2g_{YM}^2(N-b_0)\left[O_{B-C}(b_0+1,b_1-2)-2O_{B-C}(b_0,b_1)+O_{B-C}(b_0-1,b_1+2)\right] \\
\mathcal{D}O_{D-E}(b_0,b_1) = &\quad -2g_{YM}^2(N-b_0)\left[O_{D-E}(b_0+1,b_1-2)-2O_{D-E}(b_0,b_1)+O_{D-E}(b_0-1,b_1+2)\right]
\end{aligned}
$$

As before, the right hand side can be seen as a lattice version of the second derivative acting on $O_{B-C}(b_0,b_1)$ and $O_{D-E}(b_0,b_1)$. The lattice is defined by the Young tableaux, in that the lattice on which the discretised second derivative is defined is given by the shape of the Young tableaux.

7.3 Four impurity case

There are nine possible operators which can be defined in this case. The operators contain four Ys, b_0 is of size $\mathcal{O}(N)$ and b_1 ranges from 0 to size $\mathcal{O}(N)$. The operators which can be defined follow:

$\chi_A(b_0, b_1) = \chi$ 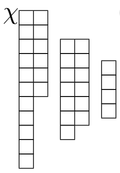 (Z, Y)

$\chi_B(b_0, b_1) = \chi$ 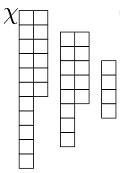 (Z, Y)

$\chi_C(b_0, b_1) = \chi$ 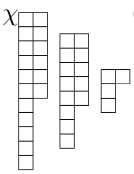 (Z, Y)

$\chi_D(b_0, b_1) = \chi$ 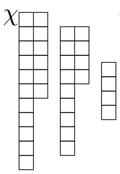 (Z, Y)

$\chi_E(b_0, b_1) = \chi$ 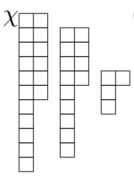 (Z, Y)

$\chi_F(b_0, b_1) = \chi$ 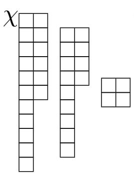 (Z, Y)

$\chi_G(b_0, b_1) = \chi$ 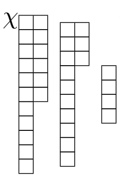 (Z, Y)

$\chi_H(b_0, b_1) = \chi$ 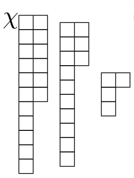 (Z, Y)

$\chi_I(b_0, b_1) = \chi$ 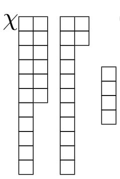 (Z, Y)

7.3.1 Spectrum

In this case the spectrum is more complex than in the previous cases. It is important to keep in mind that a_{max} is even by assumption . When $a = 0$, only the operators $\chi_I(b_0, b_1)$, $\chi_H(b_0, b_1)$ and $\chi_F(b_0, b_1)$ can be sensibly defined. When the longer column is two blocks longer than the shorter column the operators $\chi_C(b_0, b_1)$, $\chi_D(b_0, b_1)$, $\chi_E(b_0, b_1)$, $\chi_F(b_0, b_1)$, $\chi_G(b_0, b_1)$, $\chi_H(b_0, b_1)$ and

$\chi_I(b_0, b_1)$ can be defined. Thus there are ten operators which can be defined when $a < 4$. When the longer column has four or more boxes more than the shorter column, all nine operators can be defined. In total then, it is found that there are $\frac{9}{2}(a_{max} - 2) + 10 = \frac{9}{2}a_{max} + 1$ states in total.

In performing the calculation it is found that there are $\frac{5}{2}a_{max} - 1$ zero eigenvalues (corresponding to supersymmetric states). Of the $2a_{max} + 2$ non-supersymmetric states the lower eigenvalues are given by:

$$\lambda_i = 8ig_{YM}^2 \qquad i = 1, 2, \ldots, \frac{a_{max}}{2}$$

The degeneracy of the eigenvalue is three if i is odd and four if i is even. This accounts for $\frac{3}{4}a_{max} + \frac{4}{4}a_{max}$ states if a_{max} is a multiple of four, and $\frac{3}{4}(a_{max} + 2) + \frac{4}{4}(a_{max} - 2)$ states if a_{max} is not a multiple of 4.

If a_{max} is a multiple of four the remaining eigenvalues are given as follows: Above the lower lying eigenvalues just described, there are two larger eigenvalues given by $\lambda = 4a_{max}g_{YM}^2 + 8g_{YM}^2$, $\lambda = 4a_{max}g_{YM}^2 + 16g_{YM}^2$. Thereafter all the eigenvalues are non-degenerate and follow the pattern:

$$\lambda_i = 4a_{max}g_{YM}^2 + 16g_{YM}^2 + 16ig_{YM}^2 \qquad i = 1, 2, \ldots, \frac{a_{max}}{4}$$

Simply counting the states shows that all $2a_{max} + 2$ non-supersymmetric states are accounted for.

If a_{max} is not a multiple four then the remaining eigenvalues are given as follows: Above the lower lying eigenvalues there is a doubly degenerate eigenvalue $\lambda = 4a_{max}g_{YM}^2 + 8g_{YM}^2$. All the higher eigenvalues are non-degenerate and are given by:

$$\lambda_i = 4a_{max}g_{YM}^2 + 16g_{YM}^2 + 16ig_{YM}^2 \qquad i = 1, 2, \ldots, \frac{a_{max} + 2}{4}$$

Again counting the number of states shows that all the non-supersymmetric states are accounted for. The appearance of degeneracies points to the emergence of a symmetry in the large N limit.

7.4 Discretised second derivative

As before in the limit where $N - b_0 = \mathcal{O}(N)$, $b_0 = \mathcal{O}(N)$ and $b_1 = \mathcal{O}(\sqrt{N})$ the dynamics of the system simplify significantly. The previously defined normalised operators are used. In this limit the action of the dilatation operator becomes:

$$\mathcal{D}O_A(b_0,b_1) = (N-b_0)g_{YM}^2 \times O\left(\frac{1}{b_1}\right)$$

$$\begin{aligned}\mathcal{D}O_B(b_0,b_1) =& -\frac{3}{2}g_{YM}^2\,(N-b_0)\,[O_B(b_0+1,b_1-2)-2\,O_B(b_0,b_1)+O_B(b_0-1,b_1+2)]\\ &+\frac{\sqrt{3}}{2}g_{YM}^2\,(N-b_0)\,[O_C(b_0+1,b_1-2)-2O_C(b_0+1,b_1)+O_C(b_0-1,b_1+2)]\end{aligned}$$

$$\begin{aligned}\mathcal{D}O_C(b_0,b_1) =& \frac{\sqrt{3}}{2}g_{YM}^2(N-b_0)\,[O_B(b_0+1,b_1-2)-2O_B(b_0,b_1)+O_B(b_0-1,b_1+2)]\\ &-\frac{1}{2}g_{YM}^2(N-b_0)\,[O_C(b_0+1,b_1-2)-2O_C(b_0,b_1)+O_C(b_0-1,b_1+2)]\end{aligned}$$

$$\begin{aligned}\mathcal{D}O_D(b_0,b_1) =& -2g_{YM}^2\,(N-b_0)\,[O_D(b_0+1,b_1-2)-2\,O_D(b_0,b_1)+O_D(b_0-1,b_1+2)]\\ &+\frac{2}{\sqrt{3}}g_{YM}^2\,(N-b_0)\,[O_E(b_0+1,b_1-2)-2O_E(b_0+1,b_1)+O_E(b_0-1,b_1+2)]\end{aligned}$$

$$\begin{aligned}\mathcal{D}O_E(b_0,b_1) =& -2g_{YM}^2(N-b_0)\,[O_E(b_0+1,b_1-2)-2O_E(b_0,b_1)+O_E(b_0-1,b_1+2)]\\ &+\frac{2}{\sqrt{3}}g_{YM}^2(N-b_0)\,[O_D(b_0+1,b_1-2)-2O_D(b_0,b_1)+O_D(b_0-1,b_1+2)]\\ &+\frac{2\sqrt{6}}{3}g_{YM}^2(N-b_0)\,[O_F(b_0+1,b_1-2)-2O_F(b_0,b_1)+O_F(b_0-1,b_1+2)]\end{aligned}$$

$$\begin{aligned}\mathcal{D}O_F(b_0,b_1) =& -2g_{YM}^2\,(N-b_0)\,[O_F(b_0+1,b_1-2)-2\,O_F(b_0,b_1)+O_F(b_0-1,b_1+2)]\\ &+\frac{2\sqrt{6}}{3}g_{YM}^2\,(N-b_0)\,[O_E(b_0+1,b_1-2)-2O_E(b_0+1,b_1)+O_E(b_0-1,b_1+2)]\end{aligned}$$

$$\begin{aligned}\mathcal{D}O_G(b_0,b_1) =& -\frac{3}{2}g_{YM}^2\,(N-b_0)\,[O_G(b_0+1,b_1-2)-2\,O_G(b_0,b_1)+O_G(b_0-1,b_1+2)]\\ &+\frac{\sqrt{3}}{2}g_{YM}^2\,(N-b_0)\,[O_H(b_0+1,b_1-2)-2O_H(b_0+1,b_1)+O_H(b_0-1,b_1+2)]\end{aligned}$$

$$\begin{aligned}\mathcal{D}O_H(b_0,b_1) =& -\frac{1}{2}g_{YM}^2\,(N-b_0)\,[O_H(b_0+1,b_1-2)-2\,O_H(b_0,b_1)+O_H(b_0-1,b_1+2)]\\ &+\frac{\sqrt{3}}{2}g_{YM}^2\,(N-b_0)\,[O_G(b_0+1,b_1-2)-2O_G(b_0+1,b_1)+O_G(b_0-1,b_1+2)]\end{aligned}$$

$$\mathcal{D}O_I(b_0,b_1) = (N-b_0)g_{YM}^2 \times O\left(\frac{1}{b_1}\right)$$

The supersymmetric operators are annihilated by the action of the dilatation operator and are easily spotted from the above. It is clear that $O_A(b_0, b_1)$ and $O_I(b_0, b_1)$ are BPS (i.e. supersymmetric), in addition to these it can be seen that the combinations $O_B(b_0, b_1) + \sqrt{3}O_C(b_0, b_1)$, $O_D(b_0, b_1) + \sqrt{3}O_E(b_0, b_1) + \sqrt{2}O_F(b_0, b_1)$ and $O_G(b_0, b_1) + \sqrt{3}O_H(b_0, b_1)$ are all annihilated by the dilatation operator and hence are supersymmetric. Thus there are five supersymmetric operators in this limit.

Consider the operators: $\sqrt{3}O_B(b_0, b_1) - O_C(b_0, b_1) \equiv O_{B-C}(b_0, b_1)$, $\sqrt{2}O_D(b_0, b_1) - O_F(b_0, b_1) \equiv O_{D-F}(b_0, b_1)$, $O_D(b_0, b_1) - \sqrt{3}O_E(b_0, b_1) + \sqrt{2}O_F(b_0, b_1) \equiv O_{DF-E}(b_0, b_1)$ and $\sqrt{3}O_G(b_0, b_1) - O_H(b_0, b_1) \equiv O_{G-H}(b_0, b_1)$. In this limit the action of the dilatation operator becomes:

$$\begin{aligned}
\mathcal{D}O_{B-C}(b_0, b_1) &= -2g_{YM}^2(N - b_0)\left[O_{B-C}(b_0 + 1, b_1 - 2) - 2O_{B-C}(b_0, b_1) + O_{B-C}(b_0 - 1, b_1 + 2)\right] \\
\mathcal{D}O_{D-F}(b_0, b_1) &= -2g_{YM}^2(N - b_0)\left[O_{D-F}(b_0 + 1, b_1 - 2) - 2O_{D-F}(b_0, b_1) + O_{D-F}(b_0 - 1, b_1 + 2)\right] \\
\mathcal{D}O_{DF-E}(b_0, b_1) &= -4g_{YM}^2(N - b_0)\left[O_{DF-E}(b_0 + 1, b_1 - 2) - 2O_{DF-E}(b_0, b_1) + O_{DF-E}(b_0 - 1, b_1 + 2)\right] \\
\mathcal{D}O_{G-H}(b_0, b_1) &= -2g_{YM}^2(N - b_0)\left[O_{G-H}(b_0 + 1, b_1 - 2) - 2O_{G-H}(b_0, b_1) + O_{G-H}(b_0 - 1, b_1 + 2)\right]
\end{aligned}$$

This is again a lattice realisation of the second derivative, where the Young tableaux defines the lattice. The fact that the second derivative appears naturally proves that local physics appears in this limit. Also because the two threebranes are distinguishable in this limit, the radius of the three branes (which are associated with the length of the two columns of the Yong tableaux) are easily identified.

Chapter 8

Interpretation of Results

The action of the Dilation operator on two classes of restricted Schur polynomial with two columns containing $\mathcal{O}(N)$ Zs and three or four Ys respectively was calculated in the large N limit (the results are included in Appendix A). The dilatation operator was then numerically diagonalised to find the anomalous dimensions of the operators involved. A simplifying limit where $N-b_0=\mathcal{O}(N)$, $b_0=\mathcal{O}(N)$ and $b_1=\mathcal{O}(\sqrt{N})$ was investigated in detail for the cases where the operators involved had three or four impurities, and a review was given of the work done in [18] for the case where the operators involved had two impurities.

Consider the action of the dilatation operator in the limit where $N-b_0=\mathcal{O}(N)$, $b_0=\mathcal{O}(N)$ and $b_1=\mathcal{O}(\sqrt{N})$. The dynamics simplify significantly, allowing the BPS operators to be found by inspection for the cases investigated. For operators that were built with two impurities, it was found that there were three BPS states corresponding to $O_A(b_0,b_1)$, $O_B(b_0,b_1)$ and $O_D(b_0,b_1)+O_E(b_0,b_1)$. For operators built with three impurities it was found that there were four BPS states corresponding to $O_A(b_0,b_1)$, $O_F(b_0,b_1)$, $O_B(b_0,b_1)+\sqrt{2}O_C(b_0,b_1)$ and $O_D(b_0,b_1)+\sqrt{2}O_E(b_0,b_1)$. For operators built using four impurities it was found that there were five BPS states, given by:$O_A(b_0,b_1)$, $O_I(b_0,b_1)$, $O_B(b_0,b_1)+\sqrt{3}O_C(b_0,b_1)$, $O_D(b_0,b_1)+\sqrt{3}O_E(b_0,b_1)+\sqrt{2}O_F(b_0,b_1)$ and $O_G(b_0,b_1)+\sqrt{3}O_H(b_0,b_1)$.

It is easy to see that in the aforementioned simplifying limit, the BPS operators can all be written as:

$$O_{BPS}(R, r) = \sum_s \sqrt{d_s} O_{R,(r,s)}(b_0, b_1)$$

where d_s is the dimension of irreducible representation s of S_m. It is also seen in this limit that the action of the dilatation operator on the normalised operators is that of a lattice second derivative, were the Young tableaux plays the role of the lattice. The simple wave equation which appears proves that in this limit the physics becomes local, this can also be seen by the fact that the operator mixing is limited to operators related by the movement of a single box on the Young tableaux. The giant gravitons are well separated (by $\mathcal{O}(1)$ string units) in this limit, making them distinguishable. Together with the fact that the sizes of the giant gravitons are set by the lengths of the two columns, it can be seen that the radii of the giant gravitons together with local physics in the radial direction has emerged.

Next consider the spectra of the anomalous dimensions for the investigated operators (the action of the Dilatation operator appears in Appendix A). Note that the action of the Dilatation operator is rather complex. This is not surprising as the action of the dilatation operator has been calculated in the non-planar, large N limit. As discussed previously the parameter a_{max} is kept finite to make the problem computationally tractable, however the case of interest is $a_{max} = \zeta N \to \infty$ [1]. In the rest of this chapter it is assumed that $a_{max} \to \infty$. This doesn't cause any problems, as all the features of the spectra can be written explicitly in terms of a_{max}, without any assumption on the size of a_{max}.

For the case where the operators are built out of two impurities, in the limit $a_{max} \to \infty$, it is seen that there are $\frac{1}{2}a_{max}$ non-zero eigenvalues with a constant energy level spacing $8g_{YM}^2$ between them and $\frac{3}{2}a_{max}$ zero eigenvalues. A constant energy level spacing is always associated with a harmonic oscillator. Indeed the above spectrum can be understood in terms of a system of four harmonic oscillators, where three of the harmonic oscillators have a frequency of zero and one of the four harmonic oscillators has a frequency of $8g_{YM}^2$. Note that of the four operators for two impurity case there are three (A,B and E) in which the impurities are in the fully anti-symmetric representation (the representation

[1] ζ was defined in Chapter 5.1

$s = \yng(1,1)$). One (D) of the four operators has the impurities in the fully symmetric representation ($s = \yng(2)$). To reproduce the total number of states for the two impurity case each oscillator should have $\sim \frac{a_{max}}{2}$ states.

In the case where the operators were built out of three impurities, it is seen that there are six operators. There are $2a_{max}$ zero eigenvalues in the spectrum, and there are $a_{max}+1 \to a_{max}$ non-zero eigenvalues. These non-zero eigenvalues are doubly degenerate and have a constant energy level spacing of $8g_{YM}^2$. It is clear that a system of oscillators which hopes to describe the same spectrum must have twice as many oscillators with zero energy spacing as oscillators with a frequency of $8g_{YM}^2$. As the linear part of the spectrum has a degeneracy of 2 this would indicate that in an equivalent system of oscillators there should be two oscillators with a frequency of $8g_{YM}^2$ and four oscillators with a frequency of 0. Four of the six operators defined (A,B,D and F) have the impurities in the fully anti-symmetric representation $s = \yng(1,1,1)$. The remaining two operators (C and E) have the impurities in the representation $s = \yng(2,1)$. To reproduce the total number of states for the three impurity case each oscillator should have $\sim \frac{a_{max}}{2}$ states.

Consider the case where the operators were built out of four impurities. Roughly $\frac{5}{9}$ of the states give zero eigenvalues. The linear spectrum for the non-zero eigenvalues has a degeneracy which alternates between three and four and an energy spacing of $8g_{YM}^2$. This degeneracy can be more easily understood as a spectrum with a degeneracy of three and a energy level spacing of $8g_{YM}^2$, where an additional state with energy level spacing of $16g_{YM}^2$ contributes to the spectrum. If one is to describe this in terms of an equivalent set of oscillators, it is clear that there must be a single harmonic oscillator with an energy level spacing of $16g_{YM}^2$. This single harmonic oscillator, along with three harmonic oscillators with an energy level spacing of $8g_{YM}^2$ will re-create the alternating degeneracy level structure seen. Five additional harmonic oscillators with a frequency of zero will give rise to the zero eigenvalues. Note that five of the nine operators defined (A, B, D, G and I) have the impurity states in the fully anti-symmetric representation $s = \yng(1,1,1,1)$. In three of the nine operators defined (C, E and H), the impurities are in the state $s = \yng(2,1,1)$. There is also a single operator (F) with the impurities in the state $s = \yng(2,2)$. To reproduce the total number of states for the four impurity case each oscillator should have $\sim \frac{a_{max}}{2}$ states.

From the above it appears that for any number of impurities the system investigated can be thought of in terms of harmonic oscillators. Further the possible representations in which the impurities can be organised seem to indicate the energy level spacing of the oscillators required and the number of times a representation of the impurities appears seems to indicate the number of oscillators with the corresponding energy level spacing which appear. The fully anti-symmetric representations of the impurities indicate the presence of oscillators with a frequency of 0. Representations of the impurities with a single block in the second column seem to indicate the presence of oscillators with an energy level spacing of $8g_{YM}^2$, representations of the impurities with two blocks in the second column seem to indicate the presence of oscillators with an energy level spacing of $16g_{YM}^2$. Comparing the spectrum with the results found in the limit where $N - b_0 = \mathcal{O}(N)$, $b_0 = \mathcal{O}(N)$ and $b_1 = \mathcal{O}(\sqrt{N})$, it is no surprise that the number of zero oscillators and the number of BPS states in this limit agree. This together with the fact that the number of states of each oscillator is $\sim \frac{a_{max}}{2}$ irrelevant of the case investigated lends credibility to the argument that the anomalous dimensions can be understood in terms of a set of harmonic oscillators.

Cautionary note: The operators with the impurities organised into representation s *do not* correspond to the oscillators indicated by representation s. In fact the dilatation operator acting on any of the normalised operators produces a linear combination of operators belonging to the same class. So these operators do not even have a well defined scaling dimension. This should also be apparent as in general it was found that in the radial direction the BPS operators corresponded to a linear combination of the Os. Further it is found that only lengthy combinations of the Os have a well defined scaling dimension and can produce a spectrum. All that is claimed here is that the organisation of the impurities into the possible representations of s gives a way to read off the number of oscillators and their frequency. There is no further correspondence between the oscillators and the restricted Schur polynomial operators.

Following the above, it is easy to guess the results for a general number of impurities. Imagine the calculation is carried out for the case where the operators are built out of m impurities. Notice that it is always possible to put the impurities in the fully anti-symmetric representation of S_m (s is the representation of S_m), regardless of how they are arranged in representation R[2] of S_{m+n}. The impurities may be arranged in R in any of the following ways[3]: $(0,m)$, $(1,m-1)$, $\ldots$, $(m,0)$. Clearly then, given m impurities there will be $m+1$ operators where s is the fully anti-symmetric representation. Further these anti-symmetric representations indicate the presence of oscillators with a frequency of 0. If the representation s has a single box in the second column, then the evidence points at a oscillator frequency of $8g_{YM}^2$. Looking at R, it is clear that $(0,m)$ and $(m,0)$ cannot subduce a representation where s has a single box in the second column. Hence there are $m-1$ operators where s has a single block in the second column. Similarly $(0,m)$, $(m,0)$, $(1,m-1)$ and $(m-1,1)$ cannot produce operators where there are two boxes in the second column of s . Hence there will be $m-3$ operators where s has two boxes in its second column. The results suggest that these operators indicate the presence of oscillators with a frequency of $16g_{YM}^2$.

Clearly this argument can be repeated for any number of impurities in the second column, the emerging pattern is obvious. If the number of boxes is even $m=2n$, then the pattern continues until there are n boxes in the second column, hence there are n types of oscillators (oscillators with different frequencies). If the number of boxes is odd, $m=2n+1$, then the pattern can continue until there are n boxes in the second column, hence there are n types of oscillators. It follows that given m impurities, the system is equivalent to a system of harmonic oscillators with frequency ω_i and degeneracy d_i given by:

$$\omega_i = i\times 8g_{YM}^2 \qquad d_i = m+1-2i \qquad \begin{cases} i=0,1,\ldots,\frac{m}{2} \text{ If } m \text{ is even} \\ i=0,1,\ldots,\frac{m-1}{2} \text{ If } m \text{ is odd} \end{cases}$$

It is found that $\sum_i d_i$ is equal to the number of restricted Schur polynomials which can be defined, so it is found that the above conjecture passes a simple counting test.

[2]Here the longer column of R is at least m boxes longer than the shorter column, so that the impurities are never symmetrized in R.

[3]If there are a impurities in the first column of R and b impurities in the second column of R, this will be denoted as (a,b) in the discussion which follows

For every operator there is an oscillator, the frequency of which is easily found by examining the representation into which the impurities are organised. Further, as it is known that a set of harmonic oscillators is an integrable system, the dilatation operator is integrable for the system studied here, where both planar and non-planar Feynman diagrams were summed. The result that the spectrum of anomalous dimensions can be obtained from a set of harmonic oscillators is indeed powerful. This is because the alternative of calculating the action of the dilatation operator and diagonalising it is by no means straightforward (see Appendix A).

How can these results be interpreted in the dual IIB string theory? Recall that the restricted Schur polynomials studied in this dissertation are dual to excited giant graviton systems and the conformal dimension of an operator in the CFT is dual to the energy of the operator's dual in the string theory. In terms of giant gravitons in the dual string theory then, the results show a connection between excited giant gravitons and harmonic oscillators. Further it is only the two giant system and the excitations (studied here) thereof that are related to the found set of harmonic oscillators. For example, systems of giant gravitons interacting with a single graviton are not included here, as these systems would correspond to an operator labelled by Young tableaux with a small third column ($\mathcal{O}(1)$ boxes). These operators were shown to decouple in the large N limit.

It appears natural that the oscillators which describe the system of excited giant gravitons arise from the quantisation of the possible excitation modes of the giant graviton system. It should then be possible to construct classical membrane geometries from coherent states of the oscillators uncovered. Given a thorough understanding of the vibrational modes of giant graviton systems, one could then compare observables of the coherent states with observables of the membrane geometries on the gravity side of the correspondence. Such an analysis could be used as a test of the proposed modes of excitation for the giant graviton system and could provide valuable insight into systems of interacting giant gravitons.

A previous connection between the geometry of giant gravitons and harmonic oscillators was uncovered in [22, 23, 24] (following on the work done in [19]).

The harmonic oscillators discussed in [22, 23, 24] are for all the $\frac{1}{2}$, $\frac{1}{4}$ and some of the $\frac{1}{8}$ BPS states, so the space of states which connects to harmonic oscillators is enormous. The research presented in this dissertation differs in two significant ways. Firstly it is *only* the two giant system and excitations thereof which are captured in this dissertation, as opposed to a huge space of states (see the above discussion) and secondly the connection with harmonic oscillators is found to hold for non-BPS states.

As powerful as these results are they are limited in a number of ways. The most obvious shortcoming of this investigation is the rather artificial difference in treatment between the Y "impurities" and the Zs. This is obviously unwanted because $N = 4$ Super Yang-Mills exhibits $SU(4)$ symmetry. The Ys and Zs should then be treated equally, as the $SU(4)$ group contains a $U(2)$ subgroup which will mix the Zs and Ys. Further investigation should show some manifestation of the $U(2)$ symmetry. Further than this one would hope to repeat the calculation for the case where all three matrix fields (X, Y and Z) are included, in which case more of the global symmetries in $N = 4$ Super Yang-Mills should become apparent.

The results presented above suggest further investigation in the following directions:

- Is it possible to prove the conjectured one-loop results? Certainly the simplicity of the results would suggest this.
- How do higher loop corrections influence the spectrum?
- What happens to a more general system, where the Young tableaux have more than two columns, and the Schur polynomials are built out of more than two matrix fields?

Appendix A

Dilatation Operator for Three or Four impurities

For the dilatation operator for the case of two impurities see [18]. In what follows:

$$DO = g_{YM}^2 \hat{D}O\,.$$

A.1 Three Impurities

$$\hat{D}O_A(b_0,b_1) = \sqrt{(N-b_0-b_1-2)\,(N-b_0+1)}\left[4\,b_1\sqrt{\frac{b_1+4}{b_1+2}}\frac{1}{(b_1+2)\,(b_1+3)}O_B(b_0,b_1)\right.$$

$$-2\sqrt{\frac{b_1+4}{b_1+2}}\sqrt{2}\frac{1}{(b_1+2)}O_C(b_0,b_1)+8\sqrt{\frac{(b_1+4)\,(b_1+1)}{(b_1+2)\,(b_1+3)}}\frac{1}{(b_1+3)\,(b_1+2)}O_D(b_0-1,b_1+2)$$

$$\left.+2\sqrt{\frac{(b_1+4)\,(b_1+1)}{(b_1+3)\,(b_1+2)}}\frac{\sqrt{2}}{(b_1+3)\,(b_1+2)}O_E(b_0-1,b_1+2)\right]+(N-b_0-b_1-2)\left[\frac{12}{(b_1+2)\,(b_1+3)}O_A(b_0,b_1)\right.$$

$$\left.-4\,\frac{\sqrt{(b_1+1)\,(b_1+3)}\,(b_1+5)}{(b_1+3)^2\,(b_1+2)}O_B(b_0-1,b_1+2)+2\,\frac{\sqrt{(b_1+1)\,(b_1+3)}\sqrt{2}}{(b_1+3)^2}O_C(b_0-1,b_1+2)\right]$$

$$\hat{D}O_B(b_0,b_1) = \sqrt{(N-b_0-b_1-1)\,(N-b_0)}\left[-\frac{4}{3}\sqrt{\frac{(b_1+2)\,(b_1-1)}{b_1\,(b_1+1)}}\frac{(b_1-2)\,(b_1+3)}{b_1\,(b_1+1)}O_B(b_0+1,b_1-2)\right.$$

$$+\frac{2}{3}\,\frac{b_1+3}{b1}\sqrt{\frac{(b_1+2)\,(b_1-1)}{(b_1+1)\,b_1}}\sqrt{2}O_C(b_0+1,b_1-2)-\frac{32}{3}\,\frac{{b_1}^2+2\,b_1-3}{b_1(b_1+1)(b_1+2)^2}\sqrt{\frac{b_1+2}{b_1}}O_D(b_0,b_1)$$

$$-\frac{2\sqrt{2}}{3}\sqrt{\frac{b_1+2}{b_1}}\frac{(b_1+3)(3b_1-2)}{b_1(b_1+2)(b_1+1)}O_E(b_0,b_1)+8\sqrt{\frac{(b_1+3)\,b_1}{(b_1+2)\,(b_1+1)}}\frac{1}{(b_1+1)\,(b_1+2)}O_F(b_0-1,b_1+2)\Bigg]$$

$$+\sqrt{(N-b_0-b_1-2)\,(N-b_0+1)}\left[\frac{2}{3}\sqrt{\frac{(b_1+4)\,(b_1+1)}{(b_1+2)\,(b_1+3)}}\frac{\sqrt{2}b_1}{(b_1+3)}O_C(b_0-1,b_1+2)\right.$$

$$-\frac{4}{3}\sqrt{\frac{(b_1+4)\,(b_1+1)}{(b_1+3)\,(b_1+2)}}\frac{(b_1+5)\,b_1}{(b_1+3)\,(b_1+2)}O_B(b_0-1,b_1+2)$$

$$\left.+4\sqrt{\frac{b_1+4}{b_1+2}}\frac{b_1}{(b_1+3)\,(b_1+2)}O_A(b_0,b_1)\right]+(N-b_0-b_1-1)\left[-4\sqrt{\frac{b_1-1}{b_1+1}}\frac{(b_1+3)}{(b_1+1)\,b_1}O_A(b_0+1,b_1-2)\right.$$

$$+\frac{4}{3}\,\frac{(b_1+3)(b_1^3+5b_1^2+8b_1-12)}{(b_1+1)b_1(b_1+2)^2}O_B(b_0,b_1)-\frac{2\sqrt{2}}{3}\,\frac{(b_1^2+2b_1-4)(b_1+3)}{(b_1+1)(b_1+2)^2}O_C(b_0,b_1)$$

$$\left.-\frac{8}{3}\sqrt{\frac{b_1+3}{b_1+1}}\frac{(b_1+4)\,b_1}{(b_1+2)^2\,(b_1+1)}O_D(b_0-1,b_1+2)+\frac{4}{3}\,\sqrt{2}\sqrt{\frac{b_1+3}{b_1+1}}\frac{b_1}{(b_1+2)^2}O_E(b_0-1,b_1+2)\right]$$

$$+(N-b_0+1)\left[\frac{4}{3}\,\frac{(b_1+4)\,{b_1}^2}{(b_1+3)\,(b_1+2)^2}O_B(b_0,b_1)+\frac{8}{3}\,\frac{\sqrt{(b_1+1)\,(b_1+3)}b_1\,\,(b_1+4)}{(b_1+3)^2\,(b_1+2)^2}O_D(b_0-1,b_1+2)\right.$$

$$\left.-\frac{2}{3}\,\frac{\sqrt{2}\,(b_1+4)\,b_1}{(b_1+2)^2}O_C(b_0,b_1)+\frac{2}{3}\,\frac{\sqrt{2}\sqrt{(b_1+1)\,(b_1+3)}b_1\,\,(b_1+4)}{(b_1+3)^2\,(b_1+2)^2}O_E(b_0-1,b_1+2)\right]$$

$$\hat{D}O_C(b_0,b_1)=\sqrt{(N-b_0-b_1-1)\,(N-b_0)}\left[\frac{2\sqrt{2}}{3}\,\sqrt{\frac{(b_1+2)\,(b_1-1)}{(b_1+1)\,b_1}}\frac{(b_1-2)}{b_1+1}O_B(b_0+1,b_1-2)\right.$$

$$-\frac{2}{3}\sqrt{\frac{(b_1+2)\,(b_1-1)}{(b_1+1)\,b_1}}O_C(b_0+1,b_1-2)+\frac{2\sqrt{2}}{3}\sqrt{\frac{b_1+2}{b_1}}\frac{(b_1-1)(3b_1+8)}{(b_1+1)(b_1+2)^2}O_D(b_0,b_1)$$

$$\left.-\frac{4}{3}\sqrt{\frac{b_1+2}{b_1}}\frac{1}{(b_1+1)(b_1+2)}O_E(b_0,b_1)+2\,\frac{\sqrt{(b_1+2)\,(b_1+3)\,(b_1+1)\,b_1}\sqrt{2}}{(b_1+1)^2\,(b_1+2)^2}O_F(b_0-1,b_1+2)\right]$$

$$+\sqrt{(N-b_0-b_1-2)\,(N-b_0+1)}\left[-2\,\frac{\sqrt{(b_1+4)\,(b_1+2)}\sqrt{2}}{(b_1+2)^2}O_A(b_0,b_1)\right.$$

$$\left.+\frac{2\sqrt{2}}{3}\sqrt{\frac{(b_1+4)\,(b_1+1)}{(b_1+3)\,(b_1+2)}}\frac{(b_1+5)}{(b_1+2)}O_B(b_0-1,b_1+2)-\frac{2}{3}\sqrt{\frac{(b_1+4)\,(b_1+1)}{(b_1+2)\,(b_1+3)}}O_C(b_0-1,b_1+2)\right]$$

$$+(N-b_0-b_1-1)\left[2\sqrt{\frac{b_1-1}{b_1+1}}\sqrt{2}\frac{1}{b_1+1}O_A(b_0+1,b_1-2)\right.$$

$$-\frac{2\sqrt{2}}{3}\,\frac{(b_1^2+2b_1-4)(b_1+3)}{(b_1+1)(b_1+2)^2}O_B(b_0,b_1)+\frac{2}{3}\,\frac{b_1(b_1^2+2b_1-1)}{(b_1+1)(b_1+2)^2}O_C(b_0,b_1)$$

$$\left.-\frac{2}{3}\,\sqrt{2}\sqrt{\frac{b_1+3}{b_1+1}}\frac{(b_1+4)\,b_1}{(b_1+2)^2\,(b_1+1)}O_D(b_0-1,b_1+2)+\frac{2}{3}\sqrt{\frac{b_1+3}{b_1+1}}\frac{b_1}{(b_1+2)^2}O_E(b_0-1,b_1+2)\right]$$

$$+(N-b_0+1)\left[-\frac{2}{3}\,\frac{\sqrt{2}\,(b_1+4)\,b_1}{(b_1+2)^2}O_B(b_0,b_1)+\frac{2}{3}\,\frac{(b_1+4)\,(b_1+3)}{(b_1+2)^2}O_C(b_0,b_1)\right.$$

$$\left.-\frac{4}{3}\,\frac{\sqrt{2}\sqrt{(b_1+1)\,(b_1+3)}\,(b_1+4)}{(b_1+3)\,(b_1+2)^2}O_D(b_0-1,b_1+2)-\frac{2}{3}\,\frac{\sqrt{(b_1+1)\,(b_1+3)}\,(b_1+4)}{(b_1+3)\,(b_1+2)^2}O_E(b_0-1,b_1+2)\right]$$

$$\hat{D}O_D(b_0,b_1) = \sqrt{(N-b_0-b_1)(N-b_0-1)}\left[-\frac{4}{3}\sqrt{\frac{(b_1+1)(b_1-2)}{b_1(b_1-1)}}\,\frac{(b_1-3)(b_1+2)}{b_1(b_1-1)}O_D(b_0+1,b_1-2)\right.$$

$$+\frac{2}{3}\,\frac{(b_1+2)\sqrt{b_1\,(b_1-1)(b_1+1)(b_1-2)}\sqrt{2}}{b_1\,(b_1-1)^2}O_E(b_0+1,b_1-2) - 4\,\frac{(b_1+2)\sqrt{b_1\,(b_1-2)}}{{b_1}^2(b_1-1)}O_F(b_0,b_1)\Bigg]$$

$$+\sqrt{(N-b_0-b_1-1)(N-b_0)}\left[\frac{8}{b_1(b_1+1)}\sqrt{\frac{(b_1+2)(b_1-1)}{(b_1+1)b_1}}O_A(b_0+1,b_1-2)\right.$$

$$+\frac{2\sqrt{2}}{3}\,\frac{\sqrt{b_1(b_1+2)}(b_1-1)(3b_1+8)}{(b_1+1)(b_1+2)^2b_1}O_C(b_0,b_1) - \frac{32}{3}\,\frac{(b_1^2+2b_1-3)\sqrt{b_1(b_1+2)}}{(b_1+2)^2b_1^2(b_1+1)}O_B(b_0,b_1)$$

$$-\frac{4}{3}\sqrt{\frac{b_1\,(b_1+3)}{(b_1+2)(b_1+1)}}\,\frac{(b_1-1)(b_1+4)}{(b_1+2)(b_1+1)}O_D(b_0-1,b_1+2)$$

$$+\frac{2}{3}\sqrt{\frac{b_1\,(b_1+3)}{(b_1+2)(b_1+1)}}\sqrt{2}\frac{(b_1-1)}{b_1+2}O_E(b_0-1,b_1+2)\Bigg] + (N-b_0)\left[\frac{4}{3}\frac{(b_1-1)(b_1^3+b_1^2+16)}{(b_1+1)b_1^2(b_1+2)}O_D(b_0,b_1)\right.$$

$$+\frac{8}{3}\sqrt{\frac{b_1-1}{b_1+1}}\frac{{b_1}^2-4}{b_1^2(b_1+1)}O_B(b_0+1,b_1-2) - \frac{4}{3}\sqrt{2}\sqrt{\frac{b_1-1}{b_1+1}}\frac{b_1+2}{b_1^2}O_C(b_0+1,b_1-2)$$

$$-\frac{2\sqrt{2}}{3}\,\frac{(b_1^2+2b_1-4)(b_1-1)}{(b_1+1)b_1^2}O_E(b_0,b_1) + 4\,(b_1-1)\sqrt{\frac{b_1+3}{b_1+1}}\frac{1}{(b_1+2)(b_1+1)}O_F(b_0-1,b_1+2)\Bigg]$$

$$+(N-b_0-b_1)\left[\frac{4}{3}\,\frac{(b_1-2)(b_1+2)^2}{(b_1-1)\,{b_1}^2}O_D(b_0,b_1) - \frac{2\sqrt{2}}{3}\,\frac{\left({b_1}^2-4\right)}{{b_1}^2}O_E(b_0,b_1)\right.$$

$$-\frac{8}{3}\sqrt{\frac{(b_1+1)}{(b_1-1)}}\frac{\left(b_1^2-4\right)}{{b_1}^2(b_1-1)}O_B(b_0+1,b_1-2) - \frac{2\sqrt{2}}{3}\sqrt{\frac{(b_1+1)}{(b_1-1)}}\frac{\left(b_1^2-4\right)}{{b_1}^2(b_1-1)}O_C(b_0+1,b_1-2)\Bigg]$$

$$\hat{D}O_E(b_0,b_1) = \sqrt{(N-b_0-b_1)(N-b_0-1)}\left[\frac{2\sqrt{2}}{3}\sqrt{\frac{(b_1+1)(b_1-2)}{b_1\,(b_1-1)}}\,\frac{(b_1-3)}{b_1}O_D(b_0+1,b_1-2)\right.$$

$$-\frac{2}{3}\,\frac{\sqrt{b_1\,(b_1-1)(b_1+1)(b_1-2)}}{b_1\,(b_1-1)}O_E(b_0+1,b_1-2) + 2\,\frac{\sqrt{2}\sqrt{b_1\,(b_1-2)}}{{b_1}^2}O_F(b_0,b_1)\Bigg]$$

$$+\sqrt{(N-b_0-b_1-1)(N-b_0)}\left[2\,\frac{\sqrt{2}\sqrt{(b_1+2)(b_1-1)(b_1+1)b_1}}{{b_1}^2(b_1+1)^2}O_A(b_0+1,b_1-2)\right.$$

$$-\frac{4}{3}\frac{\sqrt{b_1(b_1+2)}}{(b_1+2)(b_1+1)b_1}O_C(b_0,b_1) - \frac{2\sqrt{2}}{3}\sqrt{b_1(b_1+2)}\frac{(b_1+3)(3b_1-2)}{(b_1+1)b_1^2(b_1+2)}O_B(b_0,b_1)$$

$$+\frac{2}{3}\sqrt{\frac{b_1(b_1+3)}{(b_1+2)(b_1+1)}}\sqrt{2}\frac{b_1+4}{b_1+1}O_D(b_0-1,b_1+2) - \frac{2}{3}\sqrt{\frac{b_1\,(b_1+3)}{(b_1+1)(b_1+2)}}O_E(b_0-1,b_1+2)\Bigg]$$

$$+(N-b_0)\left[-\frac{2\sqrt{2}}{3}\,\frac{(b_1^2+2b_1-4)(b_1-1)}{(b_1+1)b_1^2}O_D(b_0,b_1)\right.$$

$$+\frac{2}{3}\,\frac{(b_1+2)(b_1^2+2b_1-1)}{(b_1+1)b_1^2}O_E(b_0,b_1) - 2\sqrt{\frac{b_1+3}{b_1+1}}\sqrt{2}\frac{1}{b_1+1}O_F(b_0-1,b_1+2)$$

$$+\frac{2}{3}\sqrt{2}\sqrt{\frac{b_1-1}{b_1+1}}\frac{b_1^2-4}{(b_1+1)b_1^2}O_B(b_0+1,b_1-2)-\frac{2}{3}\sqrt{\frac{b_1-1}{b_1+1}}\frac{b_1+2}{b_1^2}O_C(b_0+1,b_1-2)\Bigg]$$

$$+(N-b_0-b_1)\left[\frac{2}{3}\frac{\left({b_1}^2-3\,b_1+2\right)}{{b_1}^2}O_E(b_0,b_1)-\frac{2\sqrt{2}}{3}\frac{\left({b_1}^2-4\right)}{{b_1}^2}O_D(b_0,b_1)\right.$$

$$\left.+\frac{4\sqrt{2}}{3}\frac{(b_1-2)\sqrt{(b_1+1)(b_1-1)}}{{b_1}^2(b_1-1)}O_B(b_0+1,b_1-2)+\frac{2}{3}\frac{(b_1-2)\sqrt{(b_1+1)(b_1-1)}}{{b_1}^2(b_1-1)}O_C(b_0+1,b_1-2)\right]$$

$$\hat{D}O_F(b_0,b_1)=\sqrt{(N-b_0-b_1)(N-b_0-1)}\left[8\frac{\sqrt{b_1\,(b_1-1)(b_1+1)(b_1-2)}}{{b_1}^2(b_1-1)^2}O_B(b_0+1,b_1-2)\right.$$

$$+2\frac{\sqrt{2}\sqrt{b_1\,(b_1-1)(b_1+1)(b_1-2)}}{{b_1}^2(b_1-1)^2}O_C(b_0+1,b_1-2)-4\,(b_1+2)\sqrt{\frac{b_1-2}{b_1}}\frac{1}{b_1\,(b_1-1)}O_D(b_0,b_1)$$

$$\left.+2\sqrt{\frac{b_1-2}{b_1}}\sqrt{2}\frac{1}{b_1}O_E(b_0,b_1)\right]+4\frac{(b_1-3)\sqrt{(b_1+1)(b_1-1)}\,(N-b_0-1)}{b_1\,(b_1-1)^2}O_D(b_0+1,b_1-2)$$

$$-2\frac{\sqrt{(b_1+1)(b_1-1)}\sqrt{2}\,(N-b_0-1)}{(b_1-1)^2}O_E(b_0+1,b_1-2)+12\frac{N-b_0-1}{b_1\,(b_1-1)}O_F(b_0,b_1)$$

A.2 Four Impurities

$$\hat{D}O_A(b_0,b_1)=\sqrt{(N-b_0-b_1-3)(N-b_0+1)}\left[6\sqrt{\frac{b_1+5}{b_1+3}}\frac{b_1}{(b_1+4)(b_1+2)}O_B(b_0,b_1)\right.$$

$$-2\sqrt{3}\sqrt{\frac{b_1+5}{b_1+3}}\frac{1}{b_1+2}O_C(b_0,b_1)+12\frac{\sqrt{(b_1+1)(b_1+5)}}{(b_1+3)(b_1+2)(b_1+4)}O_D(b_0-1,b_1+2)$$

$$\left.+4\sqrt{3}\frac{\sqrt{(b_1+5)(b_1+1)}}{(b_1+3)(b_1+4)(b_1+2)}O_E(b_0-1,b_1+2)\right]+(N-b_0-b_1-3)\left[\frac{24}{(b_1+2)(b_1+4)}O_A(b_0,b_1)\right.$$

$$\left.-6\sqrt{\frac{b_1+1}{b_1+3}}\frac{b_1+6}{(b_1+2)(b_1+4)}O_B(b_0-1,b_1+2)+2\sqrt{3}\sqrt{\frac{b_1+1}{b_1+3}}\frac{1}{b_1+4}O_C(b_0-1,b_1+2)\right]$$

$$\hat{D}O_B(b_0,b_1)=\sqrt{(N-b_0-b_1-2)(N-b_0)}\left[\frac{\sqrt{3}}{2}\sqrt{(b_1+3)(b_1-1)}\frac{b_1+4}{b_1(b_1+1)}O_C(b_0+1,b_1-2)\right.$$

$$-\frac{3}{2}\frac{\sqrt{(b_1+3)(b_1-1)}}{(b_1+1)(b_1+2)}\frac{(b_1+4)(b_1-2)}{b_1}O_B(b_0+1,b_1-2)+3\frac{(b_1+4)(b_1-1)(b_1-6)}{b_1(b_1+3)(b_1+2)^2}\sqrt{\frac{b_1+3}{b_1+1}}O_D(b_0,b_1)$$

$$\left.-\sqrt{3}\frac{(b_1+4)(3b_1-2)}{b_1(b_1+2)^2}\sqrt{\frac{b_1+3}{b_1+1}}O_E(b_0,b_1)+\frac{2b_1(b_1+4)}{(b_1+1)(b_1+3)(b_1+2)^2}\left(9O_G(b_0-1,b_1+2)+\sqrt{3}O_H(b_0-1,b_1+2)\right)\right]$$

$$+\sqrt{(N-b_0-b_1-3)(N-b_0+1)}\left[-\frac{3}{2}\sqrt{(b_1+5)(b_1+1)}\frac{b_1(b_1+6)}{(b_1+3)(b_1+2)(b_1+4)}O_B(b_0-1,b_1+2)\right.$$

$$\left.+\frac{\sqrt{3}}{2}\sqrt{(b_1+5)(b_1+1)}\frac{b_1}{(b_1+3)(b_1+4)}O_C(b_0-1,b_1+2)+6\sqrt{(b_1+5)(b_1+3)}\frac{b_1}{(b_1+2)(b_1+3)(b_1+4)}O_A(b_0,b_1)\right]$$

$$+(N-b_0-b_1-2)\left[-6\sqrt{\frac{b_1-1}{b_1+1}}\frac{b_1+4}{b_1(b_1+2)}O_A(b_0+1,b_1-2)+\frac{3}{2}\frac{(b_1^3+7b_1^2+22b_1-24)(b_1+4)}{b_1(b_1+2)^2(b_1+3)}O_B(b_0,b_1)\right.$$

$$-\frac{\sqrt{3}}{2}\frac{(b_1^2+3b_1-6)(b_1+4)}{(b_1+2)^2(b_1+3)}O_C(b_0,b_1)-6\sqrt{\frac{b_1+3}{b_1+1}}\frac{b_1(b_1+5)(b_1+4)}{(b_1+2)^2(b_1+3)^2}O_D(b_0-1,b_1+2)$$

$$\left.+\sqrt{12}\sqrt{(b_1+3)(b_1+1)}\frac{b_1(b_1+4)}{(b_1+3)^2(b_1+2)^2}O_E(b_0-1,b_1+2)\right]+(N-b_0+1)\left[\frac{3}{2}\frac{b_1^2(b_1+5)}{(b_1+2)(b_1+3)(b_1+4)}O_B(b_0,b_1)\right.$$

$$-\frac{\sqrt{3}}{2}\frac{(b_1+5)b_1}{(b_1+2)(b_1+3)}O_C(b_0,b_1)+3\sqrt{(b_1+3)(b_1+1)}\frac{b_1(b_1+5)}{(b_1+3)^2(b_1+4)(b_1+2)}O_D(b_0-1,b_1+2)$$

$$\left.+\sqrt{3}\sqrt{(b_1+3)(b_1+1)}\frac{b_1(b_1+5)}{(b_1+3)^2(b_1+2)(b_1+4)}O_E(b_0-1,b_1+2)\right]$$

$$\hat{D}O_C(b_0,b_1)=\sqrt{(N-b_0-b_1-2)(N-b_0)}\left[\frac{\sqrt{3}}{2}\sqrt{(b_1-1)(b_1+3)}\frac{b_1-2}{(b_1+1)(b_1+2)}O_B(b_0+1,b_1-2)\right.$$

$$-\frac{1}{2}\sqrt{(b_1+3)(b_1-1)}\frac{1}{b_1+1}O_C(b_0+1,b_1-2)+\frac{1}{\sqrt{3}}\sqrt{\frac{b_1+3}{b_1+1}}\frac{(b_1-1)(5b_1+18)}{(b_1+3)(b_1+2)^2}O_D(b_0,b_1)$$

$$+\sqrt{\frac{b_1+3}{b_1+1}}\frac{3b_1-2}{(b_1+2)^2}O_E(b_0,b_1)+2\sqrt{3}\frac{b_1(b_1+4)}{(b_1+1)(b_1+2)^2(b_1+3)}O_G(b_0-1,b_1+2)$$

$$\left.-\frac{4\sqrt{6}}{3}\sqrt{\frac{b_1+3}{b_1+1}}\frac{1}{b_1+2}O_F(b_0,b_1)+2\;\frac{(3b_1^2+12b_1+8)}{(b_1+3)(b_1+1)(b_1+2)^2}O_H(b_0-1,b_1+2)\right]$$

$$+\sqrt{(N-b_0-b_1-3)(N-b_0+1)}\left[\frac{\sqrt{3}}{2}\sqrt{(b_1+5)(b_1+1)}\frac{b_1+6}{(b_1+3)(b_1+2)}O_B(b_0-1,b_1+2)\right.$$

$$\left.-\frac{1}{2}\frac{\sqrt{(b_1+5)(b_1+1)}}{(b_1+3)}O_C(b_0-1,b_1+2)\;-2\sqrt{3}\frac{\sqrt{(b_1+5)(b_1+3)}}{(b_1+3)(b_1+2)}O_A(b_0,b_1)\right]+(N-b_0-b_1-2)\times$$

$$\times\left[\sqrt{\frac{b_1-1}{b_1+1}}\frac{2\sqrt{3}}{b_1+2}O_A(b_0+1,b_1-2)-\frac{\sqrt{3}}{2}\frac{(b_1^2+3b_1-6)(b_1+4)}{(b_1+2)^2(b_1+3)}O_B(b_0,b_1)+\frac{b_1^3+3b_1^2+10b_1+32}{2(b_1+2)^2(b_1+3)}O_C(b_0,b_1)\right.$$

$$-\frac{2}{\sqrt{3}}\sqrt{\frac{b_1+3}{b_1+1}}\frac{b_1(b_1+5)(b_1+4)}{(b_1+2)^2(b_1+3)^2}O_D(b_0-1,b_1+2)-2\sqrt{(b_1+3)(b_1+1)}\frac{(b_1+4)^2}{(b_1+2)^2(b_1+3)^2}O_E(b_0-1,b_1+2)$$

$$\left.+\frac{4\sqrt{2}}{\sqrt{3}}\frac{\sqrt{(b_1+3)(b_1+1)}}{(b_1+2)(b_1+3)}O_F(b_0-1,b_1+2)\right]+(N-b_0+1)\left[-\frac{\sqrt{3}}{2}\frac{b_1(b_1+5)}{(b_1+2)(b_1+3)}O_B(b_0,b_1)\right.$$

$$+\frac{1}{2}\frac{(b_1+5)(b_1+4)}{(b_1+2)(b_1+3)}O_C(b_0,b_1)-\sqrt{3}\sqrt{(b_1+3)(b_1+1)}\frac{b_1+5}{(b_1+3)^2(b_1+2)}O_D(b_0-1,b_1+2)$$

$$\left.-\sqrt{(b_1+3)(b_1+1)}\frac{(b_1+5)}{(b_1+2)(b_1+3)^2}O_E(b_0-1,b_1+2)\right]$$

$$\hat{D}O_D(b_0,b_1)=\sqrt{(N-b_0-b_1-1)(N-b_0-1)}\left[-2\frac{(b_1^2-9)(b_1^2-4)}{b_1^2(b_1^2-1)}O_D(b_0+1,b_1-2)\right.$$

$$\left.+\frac{(b_1^2-4)(b_1+3)}{b_1^2(b_1+1)^2}\left[\frac{2(b_1+1)^2}{\sqrt{3}(b_1-1)}O_E(b_0+1,b_1-2)-\sqrt{\frac{b_1+1}{b_1-1}}\left(6O_G(b_0,b_1)+\frac{2}{\sqrt{3}}O_H(b_0,b_1)\right)\right]\right]$$

$$+3\sqrt{\frac{b_1-1}{b_1+1}}\frac{{b_1}^2+b_1-6}{b_1(b_1+1)(b_1+2)}O_G(b_0,b_1)-\sqrt{3}\sqrt{\frac{b_1-1}{b_1+1}}\frac{b_1+3}{b_1(b_1+1)}O_H(b_0,b_1)$$

$$
\begin{aligned}
&+12\frac{\sqrt{(b_1+3)(b_1-1)}}{b_1(b_1+1)(b_1+2)}O_I(b_0-1,b_1+2)\Bigg]+\sqrt{(N-b_0-b_1-2)(N-b_0)}\times\\
&\times\Bigg[-3\sqrt{(b_1+3)(b_1+1)}\frac{(b_1+4)(b_1-1)}{(b_1+1)^2b_1(b_1+2)}O_B(b_0,b_1)+\sqrt{3}\sqrt{(b_1+3)(b_1+1)}\frac{b_1-1}{(b_1+1)^2(b_1+2)}O_C(b_0,b_1)\\
&+12\frac{\sqrt{(b_1+3)(b_1-1)}}{b_1(b_1+1)(b_1+2)}O_A(b_0+1,b_1-2)-2\frac{b_1(b_1-1)(b_1+4)(b_1+5)}{(b_1+1)(b_1+3)(b_1+2)^2}O_D(b_0-1,b_1+2)\\
&+6\sqrt{\frac{b_1+1}{b_1+3}}\frac{b_1(b_1^2+3b_1-4)}{(b_1+2)^2(b_1+1)^2}O_B(b_0,b_1)+\frac{2}{\sqrt{3}}\sqrt{\frac{b_1+1}{b_1+3}}\frac{b_1(b_1^2+3b_1-4)}{(b_1+2)^2(b_1+1)^2}O_C(b_0,b_1)\\
&+\frac{2}{\sqrt{3}}\frac{b_1(b_1+4)(b_1-1)}{(b_1+3)(b_1+2)^2}O_E(b_0-1,b_1+2)\Bigg]+(N-b_0-b_1-1)\Bigg[-6\sqrt{\frac{b_1-1}{b_1+1}}\frac{b_1^3+3b_1^2-4b_1-12}{b_1^2(b_1^2-1)}O_B(b_0+1,b_1-2)\\
&-\frac{2}{\sqrt{3}}\sqrt{\frac{b_1-1}{b_1+1}}\frac{b_1^3+3b_1^2-4b_1-12}{b_1^2(b_1^2-1)}O_C(b_0+1,b_1-2)+2\frac{(b_1-2)(b_1+3)^2(b_1+2)}{b_1^2(b_1+1)^2}O_D(b_0,b_1)\\
&-\frac{2}{\sqrt{3}}\frac{(b_1-2)(b_1+3)(b_1-1)(b_1+2)}{b_1^2(b_1+1)^2}O_E(b_0,b_1)\Bigg]+(N-b_0)\Bigg[3\sqrt{\frac{b_1-1}{b_1+1}}\frac{b_1^2+b_1-6}{b_1(b_1+1)(b_1+2)}O_B(b_0+1,b_1-2)\\
&-\sqrt{3}\sqrt{\frac{b_1-1}{b_1+1}}\frac{b_1+3}{b_1(b_1+1)}O_C(b_0+1,b_1-2)+6\frac{(b_1+3)(b_1-1)}{b_1(b_1+2)(b_1+1)^2}O_D(b_0,b_1)\\
&+2\sqrt{3}\frac{(b_1+3)(b_1-1)}{(b_1+2)b_1(b_1+1)^2}O_E(b_0,b_1)\Bigg]+(N-b_0-b_1-1)\Bigg[6\frac{(b_1+3)(b_1-1)}{(b_1+1)^2b_1(b_1+2)}O_D(b_0,b_1)\\
&+2\sqrt{3}\frac{(b_1-1)(b_1+3)}{(b_1+1)^2b_1(b_1+2)}O_E(b_0,b_1)-3\sqrt{\frac{b_1+3}{b_1+1}}\frac{b_1^2+3b_1-4}{b_1(b_1+1)(b_1+2)}O_G(b_0-1,b_1+2)\\
&+\sqrt{3}\sqrt{\frac{b_1+3}{b_1+1}}\frac{(b_1-1)}{(b_1+1)(b_1+2)}O_H(b_0-1,b_1+2)\Bigg]+(N-b_0)\Bigg[2\frac{(b_1+4)(b_1-1)^2b_1}{(b_1+1)^2(b_1+2)^2}O_D(b_0,b_1)\\
&-\frac{2}{\sqrt{3}}\frac{(b_1-1)(b_1+3)b_1(b_1+4)}{(b_1+1)^2(b_1+2)^2}O_E(b_0,b_1)+6\sqrt{\frac{b_1+3}{b_1+1}}\frac{(b_1^2+3b_1-4)b_1}{(b_1+1)(b_1+2)^2(b_1+3)}O_G(b_0-1,b_1+2)\\
&+\frac{2}{\sqrt{3}}\sqrt{\frac{b_1+3}{b_1+1}}\frac{(b_1^2+3b_1-4)b_1}{(b_1+1)(b_1+2)^2(b_1+3)}O_H(b_0-1,b_1+2)\Bigg]
\end{aligned}
$$

$$
\begin{aligned}
&\hat{D}O_E(b_0,b_1)=\sqrt{(N-b_0-b_1-1)(N-b_0-1)}\Bigg[\frac{2}{\sqrt{3}}\frac{b_1^3-3b_1^2-4b_1+12}{(b_1+1)b_1^2}O_D(b_0+1,b_1-2)\\
&-2\frac{(b_1^2-4)}{b_1^2}O_E(b_0+1,b_1-2)+\frac{2\sqrt{6}}{3}\frac{b_1+2}{b_1}O_F(b_0+1,b_1-2)+\sqrt{3}\sqrt{\frac{b_1-1}{b_1+1}}\frac{(b_1-2)(3b_1+8)}{b_1^2(b_1+2)}O_G(b_0,b_1)\\
&-\sqrt{\frac{b_1-1}{b_1+1}}\frac{3b_1+8}{b_1^2}O_H(b_0,b_1)+4\sqrt{3}\frac{\sqrt{(b_1+3)(b_1-1)}}{b_1(b_1+1)(b_1+2)}O_I(b_0-1,b_1+2)\Bigg]\\
&+\sqrt{(N-b_0-b_1-2)(N-b_0)}\Bigg[-\sqrt{3}\sqrt{(b_1+1)(b_1+3)}\frac{(b_1+4)(b_1-1)}{b_1(b_1+1)^2(b_1+2)}O_B(b_0,b_1)\\
&+\sqrt{(b_1+1)(b_1+3)}\frac{b_1-1}{(b_1+2)(b_1+1)^2}O_C(b_0,b_1)+4\sqrt{3}\frac{\sqrt{(b_1-1)(b_1+3)}}{b_1(b_1+1)(b_1+2)}O_A(b_0+1,b_1-2)\\
&-2\sqrt{3}\sqrt{(b_1+3)(b_1+1)}\frac{b_1(b_1+4)}{(b_1+1)^2(b_1+2)^2}O_B(b_0,b_1)\\
&+2\sqrt{(b_1+1)(b_1+3)}\frac{b_1^2}{(b_1+2)^2(b_1+1)^2}O_C(b_0,b_1)+\frac{2}{\sqrt{3}}\frac{b_1(b_1^2+9b_1+20)}{(b_1+1)(b_1+2)^2}O_D(b_0-1,b_1+2)\\
&-2\frac{b_1(b_1+4)}{(b_1+2)^2}O_E(b_0-1,b_1+2)+\frac{2\sqrt{2}}{\sqrt{3}}\frac{b_1}{(b_1+2)}O_F(b_0-1,b_1+2)\Bigg]+(N-b_0-b_1-1)\times
\end{aligned}
$$

$$\times\left[2\sqrt{3}\sqrt{\frac{b_1-1}{b_1+1}}\frac{b_1^2-4}{b_1^2(b_1+1)}O_B(b_0+1,b_1-2)-2\sqrt{\frac{b_1-1}{b_1+1}}\frac{(b_1+2)^2}{b_1^2(b_1+1)}O_C(b_0+1,b_1-2)\right.$$
$$-\frac{2}{\sqrt{3}}\frac{(b_1-2)(b_1+3)(b_1-1)(b_1+2)}{b_1^2(b_1+1)^2}O_D(b_0,b_1)+2\frac{(b_1^4+2b_1^3+b_1^2-4)}{b_1^2(b_1+1)^2}O_E(b_0,b_1)$$
$$\left.-\frac{2\sqrt{6}}{3}\frac{b_1^2+b_1-2}{b_1(b_1+1)}O_F(b_0,b_1)\right]+(N-b_0)\left[\sqrt{3}\sqrt{\frac{b_1-1}{b_1+1}}\frac{b_1^2+b_1-6}{(b_1+2)b_1(b_1+1)}O_B(b_0+1,b_1-2)\right.$$
$$-\sqrt{\frac{b_1-1}{b_1+1}}\frac{b_1+3}{b_1(b_1+1)}O_C(b_0+1,b_1-2)+2\sqrt{3}\frac{(b_1+3)(b_1-1)}{b_1(b_1+2)(b_1+1)^2}O_D(b_0,b_1)$$
$$\left.+2\frac{(b_1+3)(b_1-1)}{b_1(b_1+2)(b_1+1)^2}O_E(b_0,b_1)\right]+(N-b_0-b_1-1)\left[2\sqrt{3}\frac{(b_1-1)(b_1+3)}{(b_1+1)^2(b_1+2)b_1}O_D(b_0,b_1)\right.$$
$$+2\frac{(b_1+3)(b_1-1)}{(b_1+1)^2b_1(b_1+2)}O_E(b_0,b_1)-\sqrt{3}\sqrt{\frac{b_1+3}{b_1+1}}\frac{b_1^2+3b_1-4}{b_1(b_1+1)(b_1+2)}O_G(b_0-1,b_1+2)$$
$$\left.+\sqrt{\frac{b_1+3}{b_1+1}}\frac{b_1-1}{(b_1+1)(b_1+2)}O_H(b_0-1,b_1+2)\right]+(N-b_0)\left[-\frac{2}{\sqrt{3}}\frac{(b_1-1)(b_1+3)b_1(b_1+4)}{(b_1+1)^2(b_1+2)^2}O_D(b_0,b_1)\right.$$
$$+2\frac{(b_1+3)(b_1^2+3b_1+4)b_1}{(b_1+1)^2(b_1+2)^2}O_E(b_0,b_1)-\frac{2\sqrt{6}}{3}\frac{(b_1+3)b_1}{(b_1+2)(b_1+1)}O_F(b_0,b_1)$$
$$\left.-2\sqrt{3}\sqrt{\frac{b_1+3}{b_1+1}}\frac{(b_1+4)b_1}{(b_1+1)(b_1+2)^2}O_G(b_0-1,b_1+2)+2\sqrt{\frac{b_1+3}{b_1+1}}\frac{b_1^2}{(b_1+2)^2(b_1+1)}O_H(b_0-1,b_1+2)\right]$$

$$\hat{D}O_F(b_0,b_1)=\sqrt{(N-b_0-b_1-1)(N-b_0-1)}\left[\frac{2\sqrt{6}}{3}\frac{b_1-2}{b_1}O_E(b_0+1,b_1-2)-2O_F(b_0+1,b_1-2)\right.$$
$$\left.+\frac{4\sqrt{6}}{3}\frac{\sqrt{(b_1-1)(b_1+1)}}{b_1(b_1+1)}O_H(b_0,b_1)\right]+\sqrt{(N-b_0-b_1-2)(N-b_0)}\Big[-2O_F(b_0-1,b_1+2)$$
$$\left.\frac{2\sqrt{2}}{\sqrt{3}}\frac{b_1+4}{b_1+2}O_E(b_0-1,b_1+2)-\frac{4\sqrt{6}}{3}\sqrt{\frac{b_1+3}{b_1+1}}\frac{1}{b_1+2}O_C(b_0,b_1)\right]+(N-b_0-b_1-1)\times$$
$$\times\left[\frac{4\sqrt{6}}{3}\sqrt{\frac{b_1-1}{b_1+1}}\frac{1}{b_1}O_C(b_0+1,b_1-2)-\frac{2\sqrt{6}}{3}\frac{b_1^2+b_1-2}{b_1(b_1+1)}O_E(b_0,b_1)+2\frac{b_1-1}{b_1+1}O_F(b_0,b_1)\right]$$
$$+(N-b_0)\left[-\frac{2\sqrt{6}}{3}\frac{(b_1+3)b_1}{(b_1+2)(b_1+1)}O_E(b_0,b_1)+2\frac{(b_1+3)}{b_1+1}O_F(b_0,b_1)\ -\frac{4\sqrt{6}}{3}\sqrt{\frac{b_1+3}{b_1+1}}\frac{1}{b_1+2}O_H(b_0-1,b_1+2)\right]$$

$$\hat{D}O_G(b_0,b_1)=\sqrt{(N-b_0-b_1)(N-b_0-2)}\left[-\frac{3}{2}\frac{\sqrt{(b_1+1)(b_1-3)}(b_1^2-2b_1-8)}{b_1(b_1-2)(b_1-1)}O_G(b_0+1,b_1-2)\right.$$
$$\left.+\frac{\sqrt{3}}{2}\frac{\sqrt{(b_1+1)(b_1-3)}(b_1+2)}{(b_1-2)(b_1-1)}O_H(b_0+1,b_1-2)\ -6\sqrt{\frac{b_1-3}{b_1-1}}\frac{(b_1+2)}{b_1(b_1-2)}O_I(b_0,b_1)\right]$$
$$+\sqrt{(N-b_0-b_1-1)(N-b_0-1)}\left[18\frac{({b_1}^2-4)}{b_1^2(b_1^2-1)}O_B(b_0+1,b_1-2)\right.$$
$$+2\sqrt{3}\frac{(b_1^2-4)}{b_1^2(b_1^2-1)}O_C(b_0+1,b_1-2)-3\sqrt{\frac{b_1-1}{b_1+1}}\frac{(b_1-2)(b_1+8)(b_1+3)}{b_1^2(b_1+2)(b_1-1)}O_D(b_0,b_1)$$
$$+\sqrt{3}\sqrt{\frac{b_1-1}{b_1+1}}\frac{(b_1-2)(3b_1+8)}{b_1^2(b_1+2)}O_E(b_0,b_1)-\frac{3}{2}\sqrt{(b_1+3)(b_1-1)}\frac{(b_1^2+2b_1-8)}{b_1(b_1+1)(b_1+2)}O_G(b_0-1,b_1+2)$$

$$+\frac{\sqrt{3}}{2}\sqrt{(b_1+3)(b_1-1)}\frac{(b_1-2)}{(b_1+1)(b_1+2)}O_H(b_0-1,b_1+2)\Bigg]+(N-b_0-b_1)\Bigg[-\frac{\sqrt{3}}{2}\frac{b_1^2-b_1-6}{b_1(b_1-1)}O_H(b_0,b_1)$$

$$-\sqrt{3}\sqrt{(b_1+1)(b_1-1)}\frac{b_1^2-b_1-6}{(b_1-2)(b_1-1)^2b_1}O_E(b_0+1,b_1-2)+\frac{3}{2}\frac{(b_1-3)(b_1+2)^2}{b_1(b_1-2)(b_1-1)}O_G(b_0,b_1)$$

$$-3\sqrt{\frac{b_1+1}{b_1-1}}\frac{b_1^2-b_1-6}{(b_1-2)(b_1-1)b_1}O_D(b_0+1,b_1-2)\Bigg]+(N-b_0-1)\Bigg[-\frac{\sqrt{3}}{2}\frac{(b_1-2)(b_1^2+b_1-8)}{b_1^2(b_1-1)}O_H(b_0,b_1)$$

$$+\frac{3}{2}\frac{(b_1-2)(b_1^3-b_1^2+6b_1+48)}{b_1^2(b_1-1)(b_1+2)}O_G(b_0,b_1)+6\sqrt{\frac{b_1-1}{b_1+1}}\frac{(b_1-2)(b_1-3)(b_1+2)}{b_1^2(b_1-1)^2}O_D(b_0+1,b_1-2)$$

$$-2\sqrt{3}\sqrt{(b_1+1)(b_1-1)}\frac{b_1^2-4}{(b_1-1)^2b_1^2}O_E(b_0+1,b_1-2)+6\sqrt{\frac{b_1+3}{b_1+1}}\frac{(b_1-2)}{b_1(b_1+2)}O_I(b_0-1,b_1+2)\Bigg]$$

$$\hat{D}O_H(b_0,b_1)=\sqrt{(N-b_0-b_1)(N-b_0-2)}\Bigg[\frac{\sqrt{3}}{2}\frac{\sqrt{(b_1+1)(b_1-3)}(b_1-4)}{(b_1-1)b_1}O_G(b_0+1,b_1-2)$$

$$-\frac{1}{2}\frac{\sqrt{(b_1+1)(b_1-3)}}{b_1-1}O_H(b_0+1,b_1-2)+2\sqrt{3}\frac{\sqrt{(b_1-1)(b_1-3)}}{b_1(b_1-1)}O_I(b_0,b_1)\Bigg]$$

$$+\sqrt{(N-b_0-b_1-1)(N-b_0-1)}\Bigg[2\sqrt{3}\frac{b_1^2-4}{b_1^2(b_1^2-1)}O_B(b_0+1,b_1-2)$$

$$+2\frac{3b_1^2-4}{b_1^2(b_1^2-1)}O_C(b_0+1,b_1-2)-\frac{2}{\sqrt{3}}\sqrt{\frac{b_1-1}{b_1+1}}\frac{b_1^3+3b_1^2-4b_1-12}{(b_1^2-1)b_1^2}O_D(b_0,b_1)$$

$$-2\sqrt{\frac{b_1-1}{b_1+1}}\frac{(b_1+2)^2}{b_1^2(b_1+1)}O_E(b_0,b_1)+\frac{4\sqrt{6}}{3}\sqrt{\frac{b_1-1}{b_1+1}}\frac{1}{b_1}O_F(b_0,b_1)$$

$$+\sqrt{\frac{b_1-1}{b_1+1}}\frac{b_1+3}{b_1(b_1+1)}\left(-\sqrt{3}O_D(b_0,b_1)-O_E(b_0,b_1)\right)$$

$$+\frac{\sqrt{3}}{2}\sqrt{(b_1+3)(b_1-1)}\frac{b_1+4}{b_1(b_1+1)}O_G(b_0-1,b_1+2)-\frac{1}{2}\sqrt{(b_1+3)(b_1-1)}\frac{1}{b_1+1}O_H(b_0-1,b_1+2)\Bigg]$$

$$+(N-b_0-b_1)\Bigg[\sqrt{3}\sqrt{\frac{b_1+1}{b_1-1}}\frac{(b_1-3)}{b_1(b_1-1)}O_D(b_0+1,b_1-2)+\sqrt{\frac{b_1+1}{b_1-1}}\frac{b_1-3}{b_1(b_1-1)}O_E(b_0+1,b_1-2)$$

$$-\frac{\sqrt{3}}{2}\frac{b_1^2-b_1-6}{b_1(b_1-1)}O_G(b_0,b_1)+\frac{1}{2}\frac{b_1^2-5b_1+6}{b_1(b_1-1)}O_H(b_0,b_1)\Bigg]+(N-b_0-1)\times$$

$$\times\Bigg[\frac{2}{\sqrt{3}}\sqrt{\frac{b_1-1}{b_1+1}}\frac{b_1^3-3b_1^2-4b_1+12}{b_1^2(b_1-1)^2}O_D(b_0+1,b_1-2)+2\frac{(b_1^2-4b_1+4)\sqrt{(b_1+1)(b_1-1)}}{b_1^2(b_1-1)^2}O_E(b_0+1,b_1-2)$$

$$-\frac{4\sqrt{6}}{3}\frac{\sqrt{(b_1+1)(b_1-1)}}{b_1(b_1-1)}O_F(b_0+1,b_1-2)-\frac{\sqrt{3}}{2}\frac{(b_1-2)(b_1^2+b_1-8)}{b_1^2(b_1-1)}O_G(b_0,b_1)$$

$$+\frac{b_1^3+3b_1^2+10b_1-16}{2b_1^2(b_1-1)}O_H(b_0,b_1)-2\sqrt{3}\sqrt{\frac{b_1+3}{b_1+1}}\frac{1}{b_1}O_I(b_0-1,b_1+2)\Bigg]$$

$$\hat{D}O_I(b_0,b_1)=\sqrt{(N-b_0-b_1)(N-b_0-2)}\Bigg[12\sqrt{(b_1+1)(b_1-3)}\frac{1}{b_1(b_1-2)(b_1-1)}O_D(b_0+1,b_1-2)$$

$$+4\sqrt{3}\frac{\sqrt{(b_1+1)(b_1-3)}}{b_1(b_1-1)(b_1-2)}O_E(b_0+1,b_1-2)-6\sqrt{\frac{b_1-3}{b_1-1}}\frac{b_1+2}{b_1(b_1-2)}O_G(b_0,b_1)$$

$$+ 2\sqrt{3}\sqrt{\frac{b_1-3}{b_1-1}}\frac{1}{b_1}O_H(b_0,b_1)\Bigg] + (N-b_0-2)\Bigg[6\frac{\sqrt{(b_1+1)(b_1-1)}(b_1-4)}{b_1(b_1-1)(b_1-2)}O_G(b_0+1,b_1-2)$$

$$-2\sqrt{3}\frac{\sqrt{(b_1+1)(b_1-1)}}{(b_1-2)(b_1-1)}O_H(b_0+1,b_1-2) + 24\frac{1}{b_1(b_1-2)}O_I(b_0,b_1)\Bigg]$$

Appendix B

Projectors

It was claimed in Chapter 6 that:

$$P_s = \frac{d_s}{m!} \sum_{\sigma \in S_m} \chi_s(\sigma) \Gamma_R(\sigma)$$

was the correct projector to use. This will be proved here. In order to prove this it will be shown that P_s squares to itself (this property immediately identifies a projector). It is claimed that this projector projects from the carrier space of R to the carrier space of (r, s). Where (r, s) is an irrep of $S_n \otimes S_m$ and R is an irrep of S_{n+m}. Recall that these projectors are only allowed to act on the subspace of R where the boxes to be removed first are labelled appropriately. Given s and t irreducible representations of S_m consider the following:

$$\begin{aligned}
&P_s P_t \\
&= \frac{d_s}{m!} \sum_{\sigma \in S_m} \chi_s(\sigma) \Gamma_R(\sigma) \frac{d_t}{m!} \sum_{\rho \in S_m} \chi_t(\rho) \Gamma_R(\rho) \\
&= \frac{d_s d_t}{(m!)^2} \sum_{\sigma, \rho \in S_m} \chi_s(\sigma) \chi_t(\rho) \Gamma_R(\sigma\rho)
\end{aligned}$$

Let $\sigma\rho = \psi \Rightarrow \rho = \sigma^{-1}\psi$, and change summation variables from ρ to ψ

$$\begin{aligned}
&= \frac{d_s d_t}{(m!)^2} \sum_{\sigma, \psi \in S_m} \chi_s(\sigma) \chi_t(\sigma^{-1}\psi) \Gamma_R(\psi) \\
&= \frac{d_s d_t}{(m!)^2} \sum_{\sigma \in S_m} [\Gamma_s(\sigma)]_{ii} [\Gamma_t(\sigma^{-1})]_{jk} \sum_{\psi \in S_m} [\Gamma_t(\psi)]_{kj} \Gamma_R(\psi)
\end{aligned}$$

Given a group G where a and b are representations of the group G, the

Fundamental Orthogonality Theorem states:

$$\sum_{\alpha \in G} [\Gamma_a(\alpha)]_{ij} [\Gamma_b(\alpha^{-1})]_{pq} = \delta_{iq} \delta_{jp} \frac{|G|}{d_a} \delta_{ab} \tag{B.1}$$

Here $|G|$ is the order of the group G and d_a is the dimension of representation a.

Using the Fundamental Orthogonality theorem and the fact that $|S_m| = m!$ gives:

$$P_s P_t = \delta st \frac{ds}{m!} \sum_{\psi \in S_m} \chi_s(\psi) \Gamma_R(\psi) = \delta_{st} P_s$$

This proves that P_s is a projector as claimed, and that the projectors projecting to different subspaces are orthogonal.

Appendix C

Intertwiners

In the new formula obtained for the dilatation operator (see chapter 5) intertwiners $I_{R'T'}$ were introduced and it was claimed that the job of these intertwiners was to glue the R' and T' subspaces together. This point will be elucidated here. Consider the first term of (5.3) [1]:

$$\sum_{\psi \in S_{n+m-1}} \sum_{R',T'} c_{RR'} Tr\Big(P_{R\to(r,s)}\big(\Gamma_{R'}(\psi)\Gamma_R((n,n+1)) - \Gamma_R((n,n+1))\Gamma_{R'}(\psi)\big)\Big)\times$$
$$\times\, Tr\Big(P_{T\to(t,u)}\big(\Gamma_T((n,n+1))\Gamma_{T'}(\psi^{-1}) - \Gamma_{T'}(\psi^{-1})\Gamma_T((n,n+1))\big)\Big)$$

Summing the repeated indicies, the first term can be written as:

$$[P_{R\to(r,s)}]_{ab}[\Gamma_R((n,n+1))]_{ca}[P_{T\to(t,u)}]_{ij}[\Gamma_T((n,n+1))]_{jk}\times$$
$$\times \sum_{\substack{\psi\in \\ S_{n+m-1}}} [\oplus_{R'} c_{RR'}\Gamma_{R'}(\psi)]_{bc}[\oplus_{T'}\Gamma_{T'}(\psi^{-1})]_{ki}$$

Consider a group element $\sigma \in S_{n+m-1}$. If S_{n+m} is represented by R and R', R'_1 and R'_2 can be subduced from R by removing a single external box of the Young tableaux, then in an appropriate basis $\Gamma_R(\sigma)$ will have the form:

$$\Gamma_R(\sigma) = \begin{bmatrix} \Gamma_{R'}(\sigma) & 0 & 0 \\ 0 & \Gamma_{R'_1}(\sigma) & 0 \\ 0 & 0 & \Gamma_{R'_2}(\sigma) \end{bmatrix}$$

The variable of summation (ψ) in the new form of the dilatation operator is an element of S_{n+m-1} and will be of the above form. Let $R' \equiv T'$ for the

[1] the factors not important for the purposes of this discussion have been dropped

following argument. Then :

$$\sum_{\substack{\psi\in\\ S_{n+m-1}}} \Big[\oplus_{R'}\ c_{RR'}\Gamma_{R'}(\psi)\Big]_{bc}\Big[\oplus_{T'}\Gamma_{T'}(\psi^{-1})\Big]_{ki} =$$

$$\begin{bmatrix} c_{RR'}\Gamma_{R'}(\psi) & 0 & 0 \\ 0 & c_{RR'_1}\Gamma_{R'_1}(\psi) & 0 \\ 0 & 0 & c_{RR'_2}\Gamma_{R'_2}(\psi) \end{bmatrix}_{bc} \begin{bmatrix} \Gamma_{T'_1}(\psi) & 0 & 0 \\ 0 & \Gamma_{T'}(\psi) & 0 \\ 0 & 0 & \Gamma_{T'_2}(\psi) \end{bmatrix}_{ki}$$

The Fundamental Orthogonality theorem (B.1) is clearly applicable to the above direct product, but only the term where $\Gamma_{R'}(\psi)$ multiplies $\Gamma_{T'}(\psi^{-1})$ contributes. Thus:

$$\sum_{\substack{\psi\in\\ S_{n+m-1}}} \Big[\oplus_{R'}\ c_{RR'}\Gamma_{R'}(\psi)\Big]_{bc}\Big[\oplus_{T'}\Gamma_{T'}(\psi^{-1})\Big]_{ki} =$$

$$\frac{(n+m-1)!}{d_{R'}} c_{RR'}\delta_{R'T'} \begin{bmatrix} 0 & 1 & 0 \\ 0 & 0 & 0 \\ 0 & 0 & 0 \end{bmatrix}_{bi} \begin{bmatrix} 0 & 0 & 0 \\ 1 & 0 & 0 \\ 0 & 0 & 0 \end{bmatrix}_{kc}$$

$$\equiv \frac{(n+m-1)!}{d_{R'}} c_{RR'}\delta_{R'T'}[I_{R'S'}]_{bi}[I_{T'R'}]_{kc}$$

The job of the intertwiners in gluing the R' and T' subspaces together is now evident.

Appendix D

A Representation of S_4

Consider the representation $\boxplus$ for S_4. The group elements of S_4 can be written in an appropriate basis as:

$$\sum_i \sum_j |i\rangle\langle i|\Gamma_R(\sigma)|j\rangle\langle j|$$

Where $|i\rangle$ and $|j\rangle$ are the basis vectors. Given the following choice of basis vectors:

$$\left|\,\begin{array}{|c|c|}\hline 4 & 3 \\ \hline 2 & 1 \\ \hline \end{array}\,\right\rangle = |1\rangle = \begin{bmatrix} 1 \\ 0 \end{bmatrix} \qquad \left|\,\begin{array}{|c|c|}\hline 4 & 2 \\ \hline 3 & 1 \\ \hline \end{array}\,\right\rangle = |2\rangle = \begin{bmatrix} 0 \\ 1 \end{bmatrix}$$

The group elements of S_4 in this representation can be written as:

$$\Gamma_{\boxplus}((1)) = \Gamma_{\boxplus}((12)(34)) = \Gamma_{\boxplus}((13)(24)) = \Gamma_{\boxplus}((14)(23)) = \begin{pmatrix} 1 & 0 \\ 0 & 1 \end{pmatrix}$$

$$\Gamma_{\boxplus}((12)) = \Gamma_{\boxplus}((34)) = \Gamma_{\boxplus}((1324)) = \Gamma_{\boxplus}((1423)) = \begin{pmatrix} 1 & 0 \\ 0 & -1 \end{pmatrix}$$

$$\Gamma_{\boxplus}((13)) = \Gamma_{\boxplus}((24)) = \Gamma_{\boxplus}((1234)) = \Gamma_{\boxplus}((1432)) = -\frac{1}{2}\begin{pmatrix} 1 & \sqrt{3} \\ \sqrt{3} & -1 \end{pmatrix}$$

$$\Gamma_{\boxplus}((14)) = \Gamma_{\boxplus}((23)) = \Gamma_{\boxplus}((1243)) = \Gamma_{\boxplus}((1324)) = \frac{1}{2}\begin{pmatrix} -1 & \sqrt{3} \\ \sqrt{3} & 1 \end{pmatrix}$$

$$\Gamma_{\boxplus}((123)) = \Gamma_{\boxplus}((134)) = \Gamma_{\boxplus}((142)) = \Gamma_{\boxplus}((243)) = -\frac{1}{2}\begin{pmatrix} 1 & -\sqrt{3} \\ \sqrt{3} & 1 \end{pmatrix}$$

$$\Gamma_{\boxplus}((132)) = \Gamma_{\boxplus}((143)) = \Gamma_{\boxplus}((124)) = \Gamma_{\boxplus}((234)) = -\frac{1}{2}\begin{pmatrix} 1 & \sqrt{3} \\ -\sqrt{3} & 1 \end{pmatrix}$$

Bibliography

[1] V. De Comarmond, R. de Mello Koch, K. Jefferies
Surprisingly Simple Spectra
JHEP **0211**, 001 (2011), [arXiv:hep-th/1012.3884v1].

[2] N. Beisert, C. Kristjansen, M. Staudacher
The Dilatation Operator of Confromal N=4 Super Yang-Mills Theory
Nucl. Phys. B **663** 131-184 (2003), [arXiv:hep-th/0303060v4].

[3] J. M. Maldacena
The large N limit of superconformal field theories and supergravity
Adv. Theor. Math. Phys. **2**, 231 (1998) [Int. J. Theor. Pys. **38**,1113 (1999)], [arXiv:hep-th/9711200].

[4] S. S. Gubser, I. R. Klebanov, A. M. Polyakov
Gauge theory correlators from non-critical string theory
Phys. Lett. B **428**, 105 (1998), [arXiv:hep-th/9802109].

[5] E. Witten
Anti-de Sitter space and holography
Adv. Theor. Math. Phys. **2**, 253 (1998), [arXiv:hep-th/9802150].

[6] L Susskind, J. McGreevy, N. Toumbas
Invasion of Giant gravitons from Anti de Sitter Space
JHEP **0006**, 008 (2000), [arXiv:hep-th/003075v4].

[7] D. Berenstein
A toy model for the AdS/CFT correspondence
JHEP **0407**, 018 (2004), [arXiv:hep-th/0403110].

[8] S. Corley, A. Jevicki, S. Ramgoolam
Exact Correlators of Giant Gravitons from Dual $N = 4$ SYM theory
Adv. Theor. Math. Phys. **5**, 809 (2002), [arXiv:hep-th/0111222v3].

[9] V. Balasubramanian, M. Berkooz, A. Naqvi,M. J. Strassler
Giant Gravitons in Conformal Field Theory
JHEP(2002)034, [arXiv:hep-th/0107119v2].

[10] R. Bhattacharyya, S. Collins and R. de Mello Koch
Exact Multi-Matrix correlators
JHEP **0803**, 044 (2008), [arXiv:0801.2061 [hep-th]].

[11] R. de Mello Koch, J. Smolic, M. Smolic
Giant gravitons -with strings attached (I)
JHEP **0706**, 074 (2007), [arXiv:hep-th/0701066].

[12] R. de Mello Koch, J. Smolic, M. Smolic
Giant gravitons -with strings attached (II)
JHEP **0709**, 049 (2007), [arXiv:hep-th/0701066].

[13] R. de Mello Koch, D. Bekker, M. Stephanou
Giant gravitons -with strings attached (III)
JHEP **0802**,029 (2008), [arXiv:hep-th/0710.5372].

[14] Y. Kimura and S. Ramgoolam
Branes, Anti-Branes and Brauer Algebras in Gauge-Gravity duality
JHEP **0711**, 078 (2007), [arXiv:hep-th/0709.2158].

[15] T. W. Brown, P. J. Heslop, S. Ramgoolam
Diagonal multi-matrix correlators and BPS operators in N=4 SYM
JHEP **0802**,030 (2008), [arXiv:hep-th/0711.0176].

[16] G. 't Hooft
A planar diagram theory for strong interactions
Nucl. Phys. B **72**,461-473,(1974).

[17] R. de Mello Koch, M. Sephanou, R. Bhattacharyya
Exact multi-Restricted Schur Polynomial Correlators
JHEP **0806**,101 (2008), [arXiv:hep-th/0805.3025v1].

[18] R. de Mello Koch, G. Mashile, N. Park
Emergent Threebrane Lattices
Phys. Rev. D **81**, 106008 (2010), [arXiv:hep-th/1004.1108].

[19] A. Mikhailov
Giant gravitons from holomorphic surfaces
JHEP **0011**, 027 (2000), [arXiv:hep-th/0010206].

[20] C. E. Beasley
BPS branes from baryons
JHEP **0211**, 015 (2002), [arXiv:hep-th/0207125].

[21] J. Kinney, J. M. Maldacena, S. Minwalla, S. Raju
An index for 4 dimensional super conformal theories
Commun. Math. Phys. **275**, 209 (2007), [arXiv:hep-th/0510251].

[22] I. Biswas, D. Gaiotto, S. Lahiri, S. Minwalla
Supersymmetric states of N = 4 Yang-Mills from giant gravitons
JHEP **0712**, 006 (2007), [arXiv:hep-th/0606087].

[23] G. Mandal, N. V. Suryanarayana
Counting 1/8-BPS dual-giants
JHEP **0703**, 031 (2007), [arXiv:hep-th/0606088].

[24] J. Pasukonis, S. Ramgoolam
From counting to construction of BPS states in N=4 SYM
arXiv:1010.1683 [hep-th].

[25] I. R. Klebanov
Absorption by Threebranes and the AdS/CFT Correspondence
[arXiv:hep-th/9908165v1].

[26] I. R. Klebanov
World Volume Approach to Absorption by Non-dilatonic Branes
Nucl. Phys. B **496** 231 (1997), [arXiv:hep-th/9702076v2].

[27] S. S. Gubser, I. R. Klebanov, A. A. Tseytlin
String Theory and Classical Absorption by Threebranes
Phys. Rev. Lett. **71** 3754 (1993), [arXiv:hep-th/9703040v1].

[28] O. Aharony, S. Gubser, J. Maldcena, H. Ooguri, Y. Oz
Large N Field Theories, String Theory and Gravity
[arXiv:hep-th/9905111v3].

[29] M. E. Peskin, D. V. Schroeder
An Introduction to Quantum Field Theory
©1995 by Perseus Books Publishing L.L.C [ISBN-0-201-50397-2].

[30] N. Beisert
The Dilatation Operator of N=4 Super Yang-Mills Theory and Integrability
[arXiv:hep-th/0407277v4].

[31] L. Susskind, E. Witten
The Holographic Bound in Anti-de Sitter Space
[arXiv:hep-th/9805114v1].

[32] J. A. Minahan
The $SU(2)$ sector in AdS/CFT
Fortsch.Phys. 53 (2005) pg. 828-838, [arXiv:hep-th/0503143v2].

[33] A. Hashimoto, S. Hirano, N. Itzhaki
Large branes in AdS and their field theory dual
JHEP **0008**, 051 (2000), [arXiv:hep-th/009019v1].

[34] M. T. Grisaru, R. C. Myers, Ø. Tafjord
SUSY and Goliath
JHEP **0008**, 040 (2000), [arXiv:hep-th/0008015v1].

[35] S. R. Das, A. Jevicki, S. D. Mathur
Vibration modes of giant gravitons
Phys. Rev. D **63** 024013 (2001), [arXiv:hep-th/009019v1].

[36] S. Mukhi
Random Matrix Models of String theory
Available URL: http://theory.tifr.res.in/∼mukhi/Physics/mukhi-anu.pdf .

[37] T. Banks, W. Fischler, S.H. Shenker, L. Susskind
M Theory As A Matrix Model: A Conjecture
Phys. Rev. D**55**, 5112-5128 (1997), [arXiv:hep-th/9610043v3].

[38] R. Gwyn *Studies in the field theory - quantum gravity correspondence* MSc Dissertation (2006), University of Witwatersrand.

[39] R. de Mello Koch
Geometries from Young Diagrams
JHEP **0811**, 061 (2008), [arXiv:hep-th/0806.0685v2].

[40] H. Lin,O. Lunin,J. Maldacena
bubbling AdS space and 1/2 BPS geometries
JHEP **0410**, 025 (2004), [arXiv:hep-th/0409174v2].

[41] R. de Mello Koch, T. K. Dey, N. Ives, M. Stephanou
Correlators Of Operators with a Large R-charge
[arXiv:hep-th/0905.2273v2].